buildings

MDPI

Article

Multi-Linear and Bi-Linear Stress–Strain Approximations for Finite Element Modelling of Extended End-Plate Moment Connections

Iman Rahchamandi [1], Mohammad Reza Tavassoli [1,*], Reza Esmaeilabadi [1] and Saeed Banihashemi [2]

[1] Department of Civil Engineering, Ro.C., Islamic Azad University, Roudehen, Iran; iman.rahchamandi@iau.ac.ir (I.R.); reza.esmaeilabadi@iau.ac.ir (R.E.)
[2] School of Built Environment, University of Technology Sydney, Ultimo, NSW 2007, Australia; saeed.banihashemi@uts.edu.au
* Correspondence: mr.tavassoli@iau.ac.ir

Abstract

This study investigates the finite element analysis (FEA) of beam-to-column bolted extended end-plate moment connections, with a focus on accurately reproducing plastic rotational stiffness. Existing FEA results for six experimentally tested connections from the literature show substantial discrepancies in the plastic range, despite acceptable elastic stiffness. These discrepancies are traced to conventional material modelling practices, where only yield and ultimate stresses are specified, engineering stress–strain data are used directly, and the minimum elongation is taken as the strain at ultimate stress. To address these limitations, the connections are re-modelled in ABAQUS using (i) a multi-linear approximation for the plastic stress–strain behaviour of mild steel plates, and (ii) a proposed bi-linear approximation that requires only measured yield and ultimate strengths but preserves the area under the reference curve. In both cases, true stress–strain values are supplied to the software for plastic analysis. These strategies reduce the average error in plastic rotational stiffness from 46–48% in the existing FEA to about 18% across all specimens, while maintaining good agreement in the elastic range. The results demonstrate that carefully constructed stress–strain approximations, combined with appropriate data formatting in ABAQUS, enable reliable validation of extended end-plate moment connection models and provide a practical basis for future parametric and design studies.

Keywords: steel structures; extended end-plate connections; bolted connections; finite element analysis; plastic behaviour approximation; multi-linear approximation; bi-linear approximation

Check for updates

Academic Editor: Salvatore Verre

Received: 28 November 2025
Revised: 17 December 2025
Accepted: 19 December 2025
Published: 5 January 2026

Copyright: © 2026 by the authors. Licensee MDPI, Basel, Switzerland. This article is an open access article distributed under the terms and conditions of the Creative Commons Attribution (CC BY) license.

1. Introduction and Background

Extended end-plate moment connections are commonly used in steel structures in view of their ability to allow fast erection of rigid joints without requiring any field welding [1]. These connections are prequalified for seismic applications and their design provisions are clearly outlined in [2,3]. Their behaviour is typically investigated using two main approaches: experimental testing and finite element analysis (FEA) [4]. While experimental testing provides benchmark data, numerical modelling offers a cost-effective alternative for evaluating connection performance and enables extensive parametric studies [5]. However, it remains essential to ensure the accuracy of FEA results and validate the software's functionality. Connection performance is typically evaluated through moment–rotation curves, as they provide a comprehensive representation of connection behaviour [6].

The earliest 3D modelling of bolted end-plate connections was carried out using eight-node sub-parametric brick elements [7,8].

A finite element modelling approach using ANSYS was studied to simulate the moment–rotation behaviour of bolted extended end-plate connections, with results validated against experimental data through both 2D and 3D analyses [9,10]. This work was later extended using 3D models to evaluate the stiffness and strength of these connections, considering the interaction between end-plates and both stiffened and unstiffened column flanges [11,12].

A 3D finite element model was adopted using ABAQUS to simulate the stiffness and strength behaviour of bolted extended end-plate connections, with results verified against experimental data to assess the accuracy of the proposed modelling approach [13].

Bolted extended end-plate connections were investigated using FEA, incorporating material nonlinearities, geometrical discontinuities, and large displacements. Comparisons with experimental results for moment–rotation curves, end-plate displacements, and bolt forces showed satisfactory agreement [14].

Experimental research was conducted on eight full-scale steel beam-to-column end-plate moment connection specimens subjected to cyclic loading. The investigated parameters included end-plate thickness, bolt diameter, end-plate stiffener, column stiffener, and the type of end-plate (flush or extended) [15]. The study was later extended by developing finite element models of the same specimens and validating the FEA results against experimental data, in terms of moment–rotation curves [16].

Current design equations for extended end-plate connections were revised to better account for prying action and enhance connection ductility. The proposed equations for prying force and bending moment were validated against finite element results, showing satisfactory accuracy [17]. The cyclic behaviour of column web panel components in bolted end-plate connections was investigated through detailed ABAQUS modelling and experimental validation. A procedure was developed to facilitate the component-based modelling of joints under cyclic loading [18].

Performance of unstiffened extended end-plate bolted beam-to-column connections was investigated under a central column removal scenario. Experimental results validated finite element models, and the study concluded that bolt strengthening is required to improve progressive collapse resistance of these connections [19].

The behaviour of extended stiffened end-plate connections was evaluated using FEA and compared based on AISC and European design criteria [20]. In a later study, the influence of rib stiffeners on the performance of extended end-plate connections, considering parameters such as thickness, slope, and constructional imperfections, was investigated [21].

A study analysing 180 configurations of stainless steel extended end-plate beam-to-column connections showed that these connections, particularly those with end-plate stiffeners, exhibit excellent ductility and rotation capacity, making them suitable for seismic applications [22].

A hysteresis envelope model for double extended end-plate bolted joints was developed based on cyclic numerical simulations, enabling more realistic representation of joint behaviour in nonlinear pushover analyses of steel frames [23].

The seismic behaviour of end-plate connections between a steel beam and the weak axis of an H-shaped column using a U-shaped connector was examined through numerical models in ABAQUS. The study evaluated the effects of connector thickness, end-plate thickness, axial compression ratio of the columns, and the linear stiffness ratio of the beam to the column, and recommended reasonable ranges for these parameters [24].

Holistically, these works focus on strength, stiffness, or parametric design where they typically use simplified material models. Furthermore, the literature is limited in system-

atically quantifying the error in plastic rotational stiffness arising solely from material modelling choices and stress–strain data format.

The application of simplified material models may lead to an underestimation of plastic stiffness. Underestimation of plastic stiffness in finite element analysis may lead to unrealistically large plastic deformations. This underestimation can result in a reduced area under the moment–rotation curve in pushover analyses and smaller enclosed areas of hysteresis loops in cyclic analyses. Consequently, the energy dissipation capacity of the connection under cyclic loading conditions, such as seismic actions, may be underestimated, which could affect the assessment of connections in practice.

Accurate definition of the mechanical properties of materials is a key factor in obtaining reliable FEA results. However, limited attention has been given to how simplified material models and data formatting choices (e.g., use of engineering instead of true stress–strain values, or the selection of ultimate strain) influence the predicted plastic rotational stiffness of extended end-plate connections. In particular, there is no systematic guidance on how to define stress–strain relationships when only yield and ultimate strengths are available, as is typical in experimental reports and design documentation. This paper addresses these gaps by:

(i) Diagnosing the sources of discrepancy between experimental and existing FEA results for six benchmark connections;
(ii) Implementing multi-linear and the proposed bi-linear approximations for the stress–strain behaviour of steel plates and bolts in ABAQUS;
(iii) Quantifying the impact of these approximations on plastic rotational stiffness.

Section 2 presents and discusses linear, bi-linear, and multi-linear approximations of the plastic stress–strain behaviour of connection components. Section 3 introduces six beam-to-column extended end-plate moment connections from [15,16] and compares their existing experimental and FEA results, highlighting the observed discrepancies. In Section 4, the previously discussed approximations are applied to define the mechanical properties of materials in the finite element models, and the resulting FEA outcomes are once again compared with experimental data. Finally, Section 5 summarizes the main conclusions of this research.

2. Materials and Methods

The overall workflow adopted in this study is summarised in the research methodology framework shown in Figure 1.

2.1. Material Modelling for Steel Plates

The process of defining elastic mechanical properties in ABAQUS software involves specifying the elasticity modulus and Poisson's ratio. By providing these two values, the analysis in the elastic region can be conducted accurately, leading to FEA results that closely align with experimental findings.

When defining the plastic behaviour in ABAQUS software, it is necessary to input the stress–strain values as pairs of numbers. If an accurate stress–strain diagram for the steel plates is available, the plastic behaviour can be defined in the software by inputting coordinates of multiple points from the diagram. If such a diagram is not available, a multi-linear approximated diagram of the stress–strain behaviour of steel can be utilised.

The steel plates used in the specimens presented in this paper are grade Q345, which has mechanical properties comparable to ASTM A572 Grade 50 [25]. Figure 2 illustrates the multi-linear approximation for stress–strain behaviour of mild steel, such as ASTM A572Gr50. This diagram is adapted from a report primarily intended to develop estimates for the average behaviour of mild structural steel for use in finite element models [26].

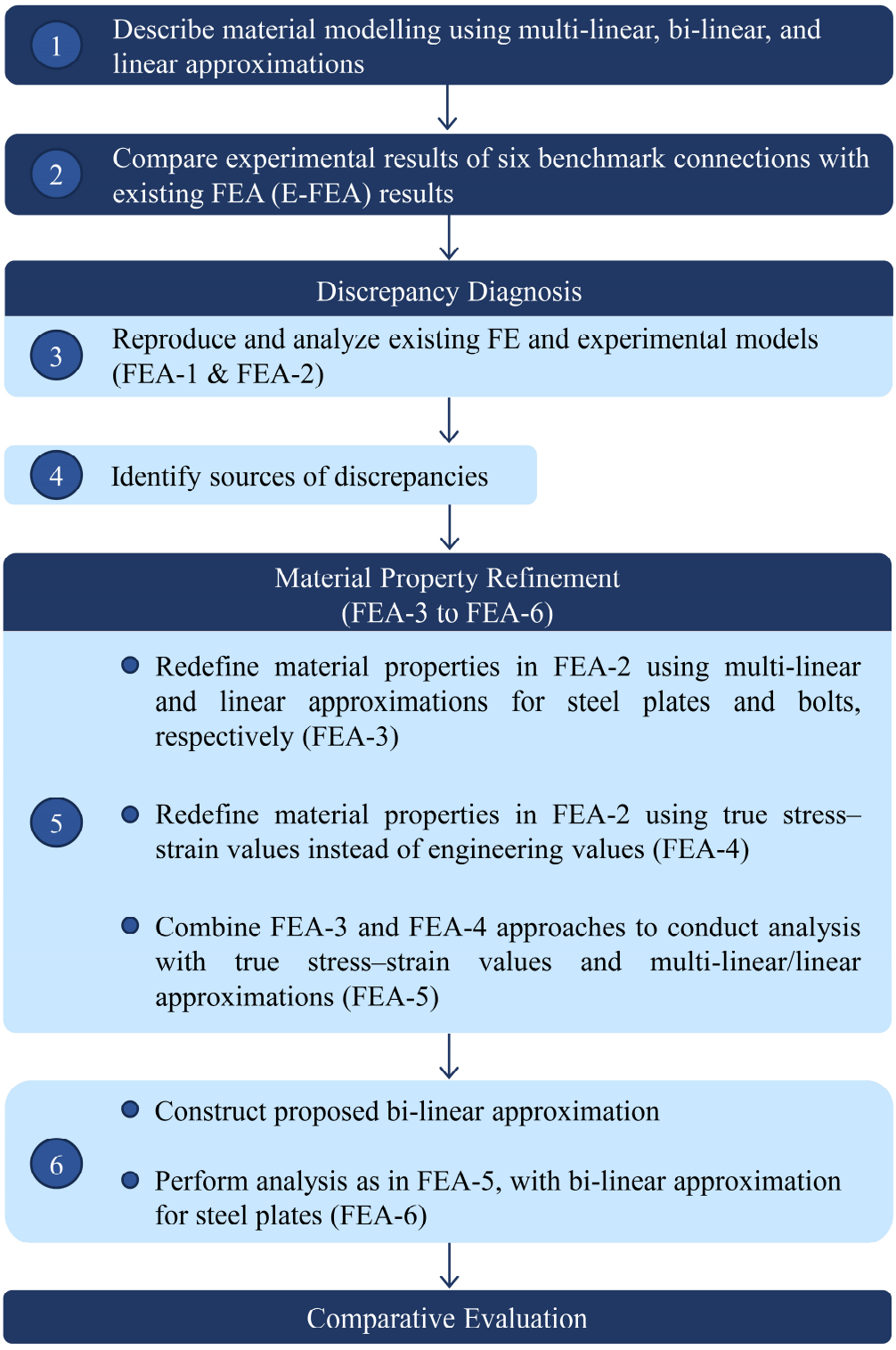


Figure 1. Research methodology framework of the study.

It is crucial to note that code minimum yield and ultimate stress values are always employed for design purposes. Nevertheless, when validating FEA results against experimental findings, it becomes essential to utilize the measured and reported values from experimental tests. Experimental tests usually provide limited data, primarily consisting of yield stress and ultimate stress values. Therefore, for a convenient and accurate definition of the mechanical properties of steel plates within the software, a practical approach

involves using the multi-linear approximation illustrated in Figure 2. This is achieved by substituting the reported values directly into this diagram.

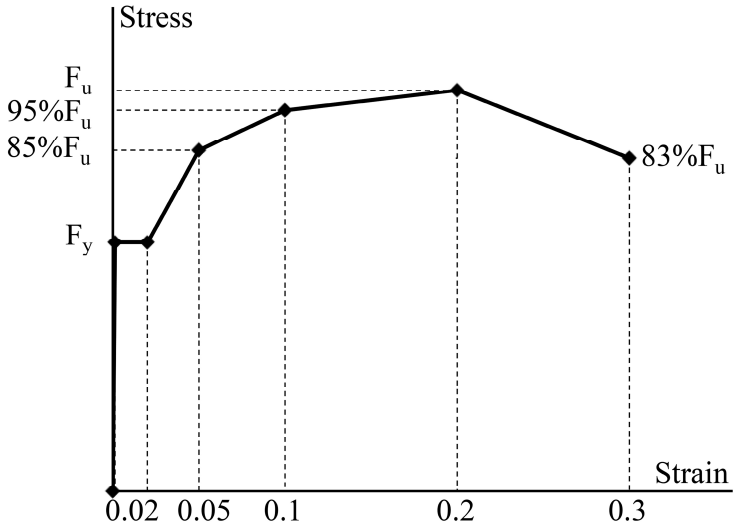
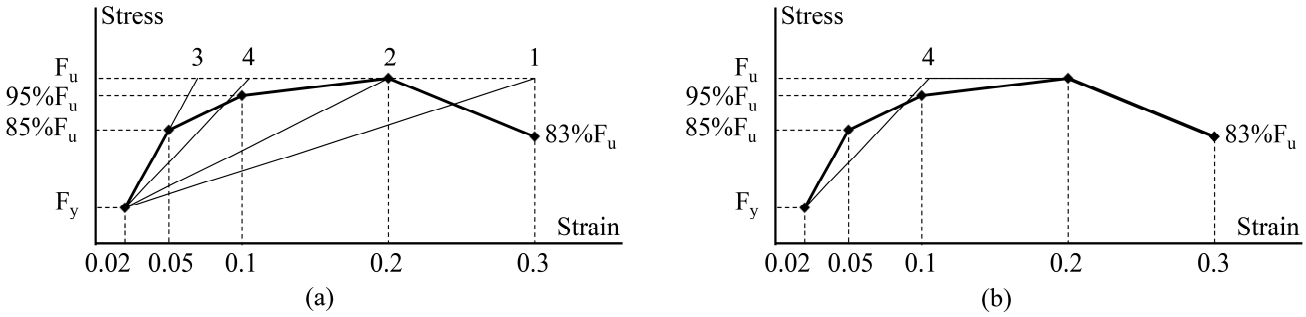


Figure 2. Multi-linear approximation for stress–strain behaviour of mild steel [26].

If it is essential to define the mechanical properties of steel plates based solely on the measured and reported yield stress and ultimate stress values, the plastic behaviour of the steel can be linearly defined using two pairs of numbers. The first pair consists of the yield stress and its corresponding plastic strain, which is zero. The stress component of the second pair is the ultimate stress, which is also known. The remaining value is the strain component of the second pair, representing the plastic strain corresponding to the ultimate stress. Selecting this value accurately is one of the primary aspects of interest in this article since an imprecise choice can lead to inaccurate FEA results.

To achieve a linear approximation for the plastic behaviour of mild steel, Figure 3a is presented. In this figure, the plastic behaviour of mild steel is depicted, derived from Figure 2, without considering the initial plastic strain and starting from a total strain of 0.02.



Original diagram: Multi-linear approximation
Linc 1: Linear approximation using elongation at rupturc
Line 2: Linear approximation using ultimate strain
Line 3: Linear approximation using initial plastic stiffness
Line 4: Middle-span linear approximation (visual reference)

Original diagram: Multi-linear approximation
Line 4: Bi-linear approximation using equal area method

Figure 3. Approximations for the plastic stress–strain behaviour of mild steel (**a**) linear (**b**) bi-linear.

If elongation at rupture is considered as the strain corresponding to the ultimate stress, the linear approximation for the plastic stress–strain behaviour of the steel plates is represented by line No. 1 in Figure 3a, which leads to a significantly lower plastic stiffness

than the actual value. As a consequence, the simulation of the steel's plastic behaviour becomes inaccurate, resulting in discrepancies between FEA and experimental results.

If the ultimate strain is considered as the strain corresponding to the ultimate stress, the linear approximation of the steel's plastic behaviour will resemble line No. 2 in Figure 3a. However, it is crucial to note that although the beginning and end points of the linear approximation coincide respectively with the yield point and ultimate point of the original diagram, the area under the linear approximation is considerably smaller than that of the original diagram. Consequently, steel plates modelled using the linear approximation (line No. 2) will exhibit lower toughness, indicating a reduced capacity to absorb energy before fracture.

If the plastic stiffness of steel throughout the plastic zone is assumed to be equal to the plastic stiffness between strain 0.02 and 0.05, the linear approximation of the plastic behaviour of steel will be represented by line No. 3 in Figure 3a. In this scenario, the plastic behaviour of the steel is modelled with a significantly higher stiffness than its actual stiffness, and concurrently, the ultimate strain is greatly reduced. Essentially, the steel's behaviour transitions from being mild to becoming brittle.

Considering line No. 4 in Figure 3a as the linear approximation of the plastic behaviour of mild steel, it is evident that this approximation also underestimates the ultimate strain of the steel. This is despite appearing to be an appropriate linear approximation as it passes through the middle span of the original diagram.

Therefore, it can be concluded that the linear approximation of the plastic stress–strain behaviour of mild steel will result in significant discrepancies when compared to the original diagram. To address this, a stiffness-free region should be incorporated at the end of the linear approximation (line No. 4). Consequently, the linear approximation of the steel plates' plastic stress–strain behaviour, shown in Figure 3a, is transformed into a bi-linear approximation, as illustrated in Figure 3b. The exact position of line No. 4 (strain corresponding to the ultimate stress) is determined by ensuring equality in the areas under the diagrams, as explained in Section 4.2.

It is important to highlight that the proposed bi-linear approximation, represented by line No. 4 in Figure 3b, accurately incorporates the following parameters: ultimate stress, ultimate strain, average plastic stiffness, and the area under the diagram in the plastic zone. Notably, although three pairs of numbers should be defined in the software for the proposed bi-linear approximation, only the yield and ultimate stress values are required.

2.2. Material Modelling for Bolts

In the connections presented in this paper, grade 10.9 bolts are utilised in addition to the aforementioned steel plates. Therefore, it is essential to obtain the approximation of the plastic stress–strain behaviour not only for the steel plates but also for the bolts.

The mechanical properties of Grade 10.9 bolts are comparable to those specified for ASTM A490M bolts [27,28]. The engineering stress–strain diagram of ASTM A490M bolts is illustrated in Figure 4a [29,30]. The available data from experimental reports regarding bolts are also usually limited to yield stress and ultimate stress. Consequently, as with steel plates, defining the plastic behaviour of bolts is feasible using multi-linear approximation, if available, or by employing bi-linear or linear approximations.

Figure 4b depicts the plastic zone presented in Figure 4a, extending from the yield to the ultimate stress point, together with its linear approximation. This approximation was established by enforcing equality between the areas under the original curve and the linear representation. Initially, the line connecting the yield and ultimate points was adopted as the approximation, and its enclosed area was compared with that of the actual curve. The approximation was subsequently shifted upward in proportion to the ratio of the two areas.

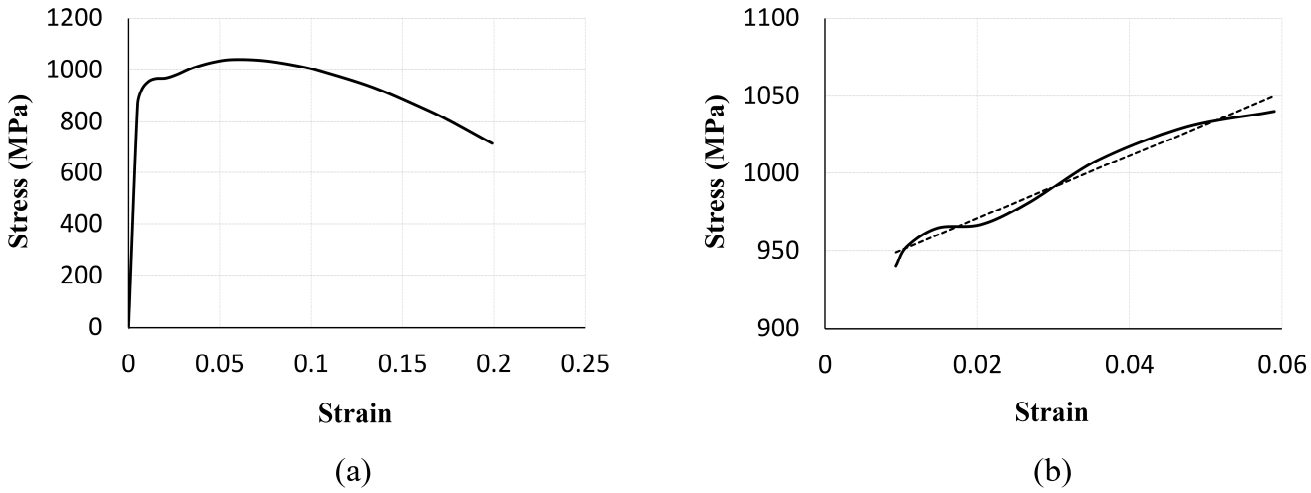


Figure 4. (**a**) Engineering stress–strain diagram for ASTM A490M bolts [29,30] (**b**) Enlarged plastic zone of (**a**) along with its linear approximation.

In this scenario, considering the close agreement between the original diagram and its linear approximation throughout the entire range, as well as the near coincidence of the start and end points of the linear approximation with the yield and ultimate points (differing by less than 1%), it is feasible to utilize the connecting line between the yield and ultimate points to define the plastic stress–strain behaviour of bolts, instead of relying on the original diagram. Consequently, a linear approximation suffices for defining the plastic behaviour of bolts with an acceptable accuracy. In this case, defining the plastic stress–strain behaviour for the software entails using two pairs of numbers: the first pair consisting of the yield stress and its corresponding plastic strain, which is zero, and the second pair comprising the ultimate stress and its corresponding plastic strain, roughly 0.05 (0.01–0.06).

The possibility of employing the linear approximation for the plastic stress–strain behaviour (a straight line connecting the yield and ultimate points) for ASTM A490M bolts stems from their brittle behaviour. Conversely, using a linear approximation for mild steels like ASTM A572Gr50 steel plates leads to notable discrepancies due to their ductile nature, causing significant plastic strains near the ultimate stress.

3. Assessment of Existing Results

3.1. Comparison of Experimental Results [15] and Existing FEA Results [16]

The core objective of this section is to identify the core causes of deviations in plastic rotational stiffness through the comparison of experimental and existing FEA results, providing a basis for the subsequent optimisation of material models. To illustrate the importance of precisely defining the mechanical properties of materials within the software when validating FEA results, this study focuses on six specific connections (JD2, JD3, JD4, JD6, JD7, and JD8), detailed in [15,16]. These connections are categorised as cantilever beam-to-column bolted extended end-plate moment connections. The existing results for these connections are provided in terms of moment–rotation diagrams. The connections were initially subjected to experimental tests [15], and their results are presented under the title "Experimental" in this paper. They were later modelled and analysed using ANSYS software [16], and the existing FEA results are presented under the title "E-FEA" in the current paper. The mechanical properties of the steel plates and bolts used in the experimental tests are outlined in Table 1, while the corresponding properties employed in the E-FEA are presented in Table 2.

Table 1. Mechanical properties of materials reported in experimental tests [15].

Material	Measured Average Yield Strength (MPa)	Measured Average Tensile Strength (MPa)	Measured Average Elastic Modulus (MPa)	Measured Bolt Average Pretension Force (kN)
Steel Plates (thickness $\leq$ 16 mm)	409	536.6	195,452	–
Steel Plates (thickness > 16 mm)	372.6	537	188,671	–
Bolts (M20)	995	1160	206,000 (Nominal)	199
Bolts (M24)	975	1188	206,000 (Nominal)	283

Table 2. Mechanical properties of materials used in E-FEA [16].

Material	Yield Strength (MPa)	Tensile Strength (MPa)	Elastic Modulus (MPa)	Bolt Pretension Force (kN)
Steel Plates (thickness $\leq$ 16 mm)	391	391	190,707	–
Steel Plates (thickness > 16 mm)	363	363	204,227	–
Bolts (M20)	–	–	–	155
Bolts (M24)	–	–	–	225
Stress–Strain Relationship for High Strength Bolts				
Stress (MPa)	0	990	1160	1160
Strain (%)	0	0.483	13.6	15

Notably, there is a distinction in the mechanical properties of the steel plates between the E-FEA and experimental tests. In the E-FEA, the steel plates are modelled as "Elastically-Perfect Plastic", whereas different properties are observed in the experimental tests. Additionally, it is worth mentioning that the pre-tensioning stress values of the bolts are reported higher in the experimental tests. This variation is attributed to stress relaxation, as stated in [15]. The experimental and E-FEA results of the connections are presented in Figure 5.

In Figure 5, it is apparent that there is initial agreement between the experimental and E-FEA results in all diagrams. However, upon closer examination, significant differences emerge. The elastic zones of both cases exhibit similar characteristics, such as the stiffness. However, in all diagrams, the E-FEA results demonstrate higher yield moment values compared to the experimental results. This discrepancy is more pronounced in connections JD2, JD6 and JD7.

The main disparity between the experimental and E-FEA results lies in the plastic performance of the connections. In all connections, the experimental diagrams exhibit a steeper slope in the plastic zone, which demonstrates higher plastic rotational stiffness. Conversely, the E-FEA diagrams display a significantly lower slope within the plastic zone. While the E-FEA diagrams show higher yield moment values than the experimental diagrams, they demonstrate lower ultimate moment values due to their limited plastic rotational stiffness. In essence, the disparity in the plastic zone between the experimental and E-FEA diagrams is partially masked by these two opposing differences.

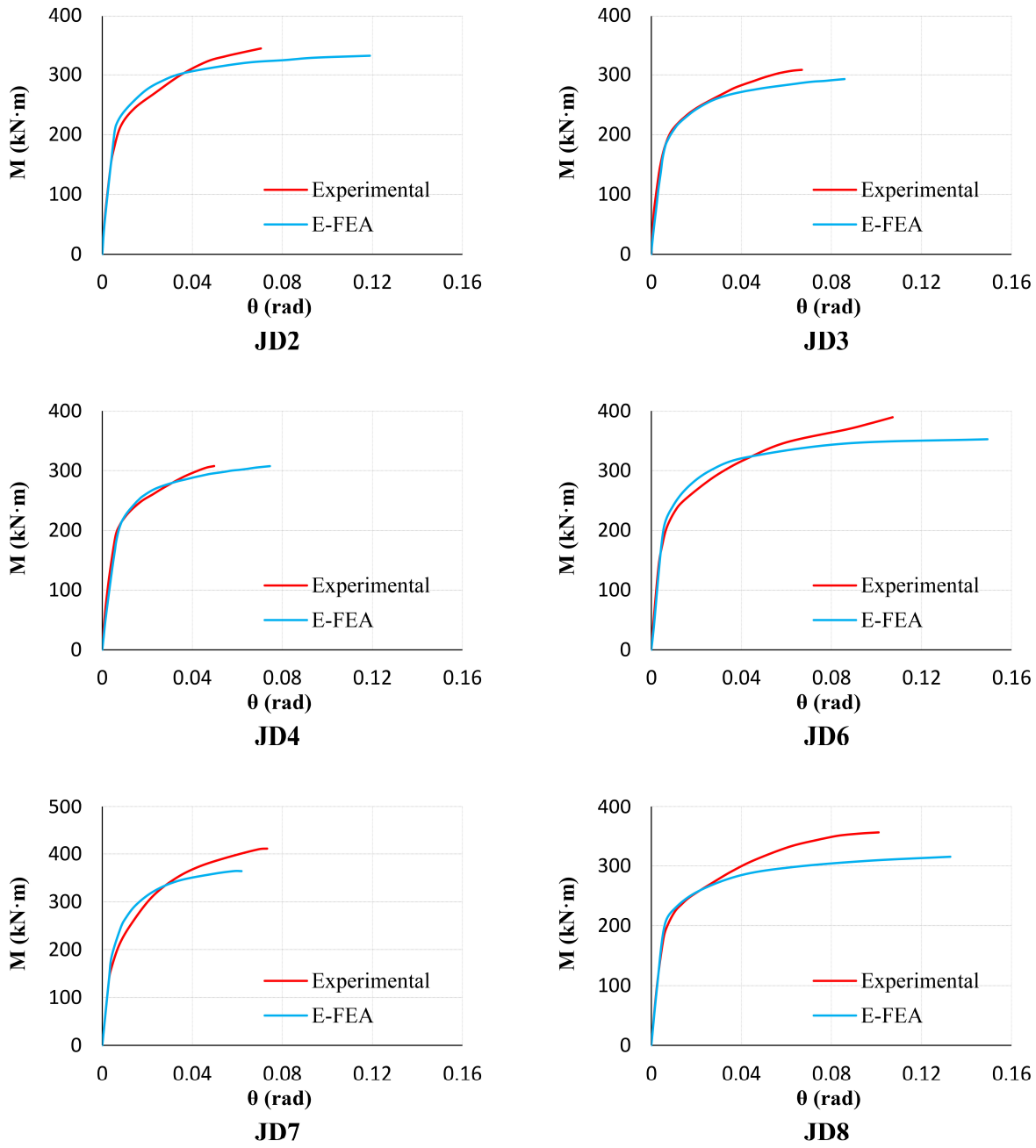


Figure 5. Experimental results [15] and E-FEA results [16].

3.2. Simulation of Existing FE Models

The utilisation of steel plates with different mechanical properties in the E-FEA is highlighted as a major factor contributing to the discrepancy in the plastic behaviour between the experimental and E-FEA results [16]. To investigate this claim, the current study conducted FEA, modelling and analysing the connections based on the mechanical properties employed in E-FEA. Connections were modelled in ABAQUS/CAE 2020 (Dassault Systèmes) using solid elements. Bolts were modelled with hexagonal heads using dimensions from [31,32]. The interface between the end-plate and the column flange was modelled using surface-to-surface contact, with a coefficient of friction of 0.44, consistent with the values reported in [16]. To ensure both accuracy and efficiency in the analysis, proper meshing was achieved by employing a substantial number of partitions. As the mesh density is not explicitly specified in [16], a limited sensitivity analysis was first conducted to evaluate the influence of mesh size, ensuring that the results remained

meaningfully comparable. The meshing of the connection sections is shown in Figure 6, and the results are presented in Figure 7 under the label "FEA-1". The dataset supporting this study is openly available in Mendeley Data [33].

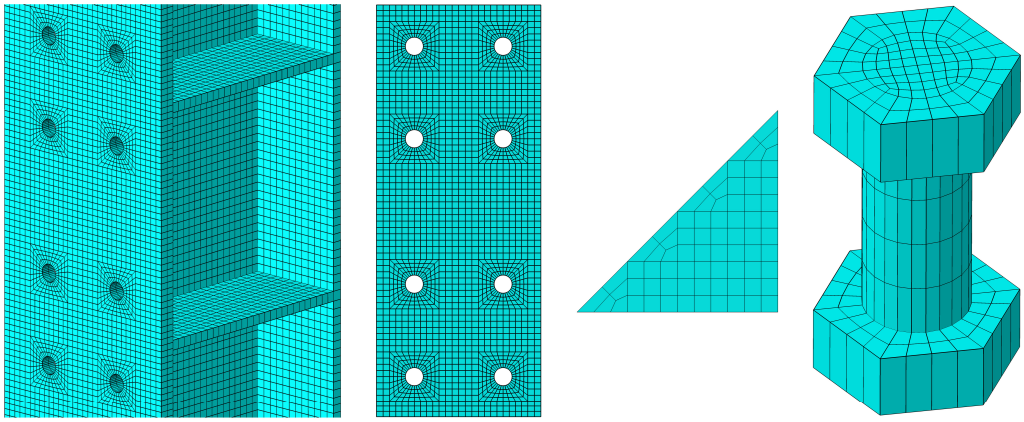


Figure 6. Structured meshing of the connection sections.

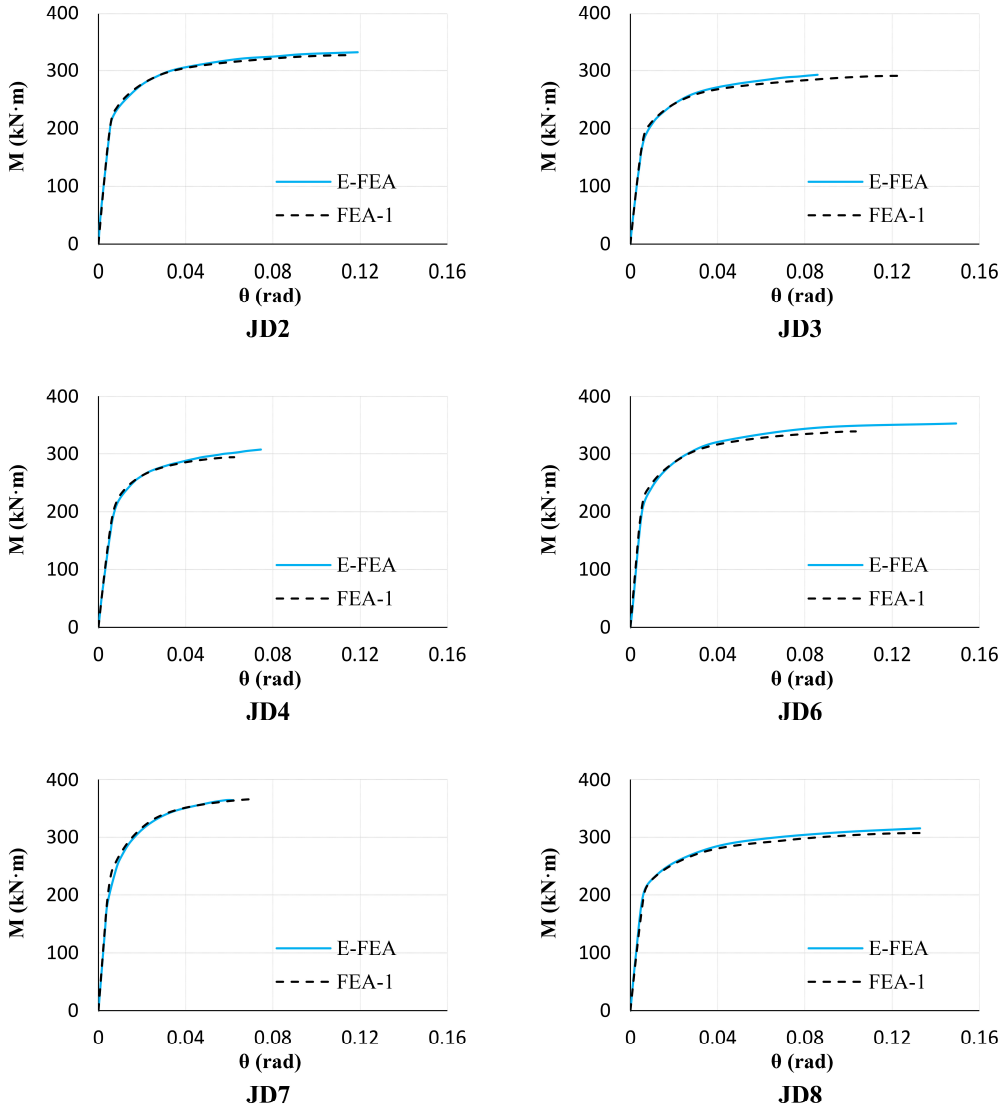


Figure 7. E-FEA results [16] and new FEA results based on E-FEA mechanical properties (FEA-1).

Figure 7 demonstrates strong agreement between the FEA results obtained in this study and the E-FEA results. This not only supports the authors' assertion regarding the use of elastically-perfect plastic steel plates in the E-FEA but also validates the accurate modelling and analysis conducted in the present research.

3.3. Simulation of Experimental Tests

To further investigate the sources of discrepancies in the E-FEA results, the connections were subsequently remodelled and reanalysed using the mechanical properties reported in the experimental tests [15]. To accurately replicate the conditions of the experimental tests reported in [15], an axial force of 485 kN was applied to the column, which had not been considered in the E-FEA. This axial force corresponds exactly to the loading applied in the reference experimental tests. The results are depicted in Figure 8, labelled as "FEA-2". Figure 8 also showcases the experimental results and the E-FEA results.

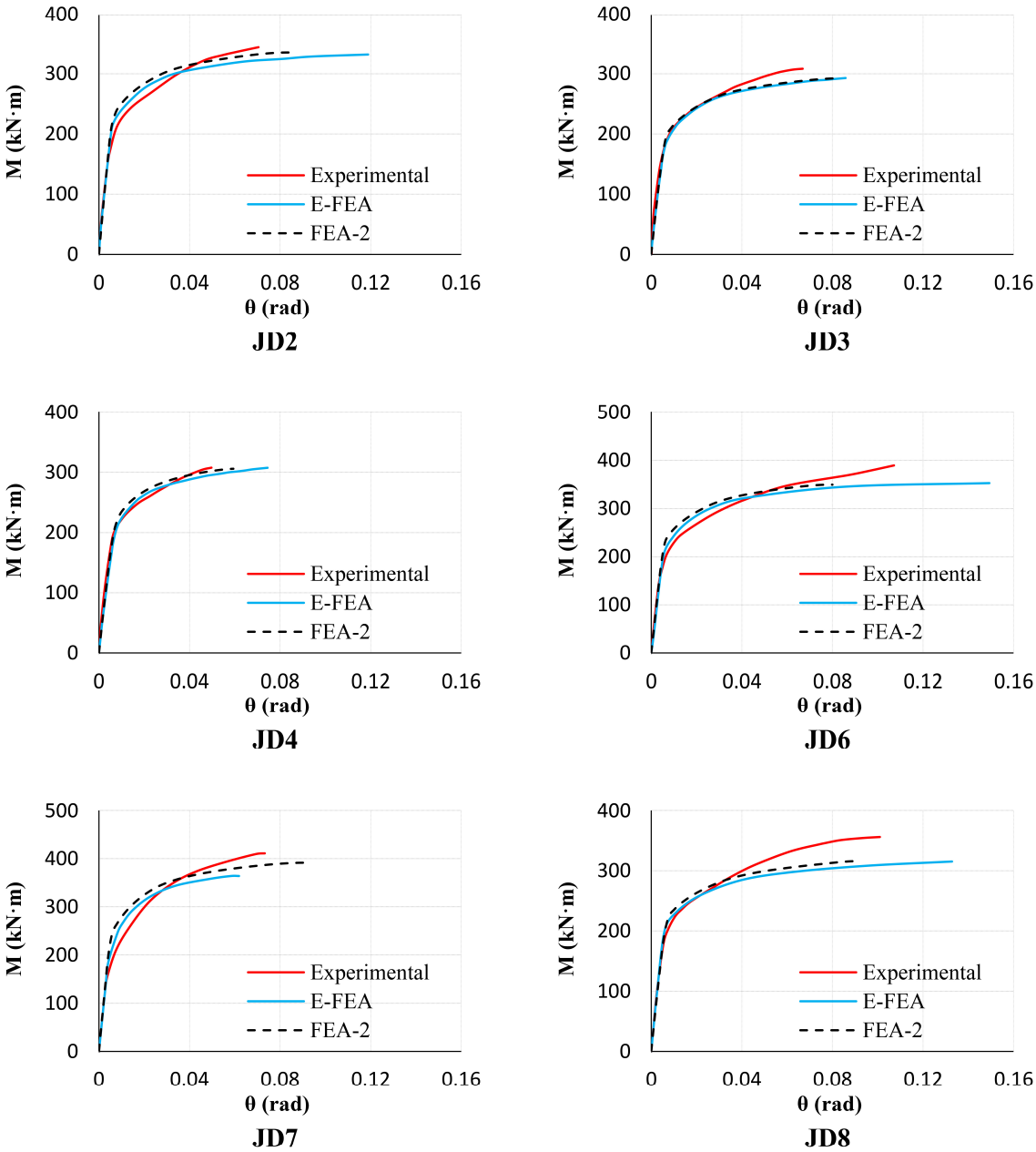


Figure 8. Experimental results [15], E-FEA results [16], and new FEA results based on experimental test mechanical properties (FEA-2).

The mechanical properties utilised in FEA-2 were taken from the experimental tests. However, Figure 8 demonstrates that the plastic behaviour of the FEA-2 results aligns more closely with the E-FEA results than with the experimental results. Notably, FEA-2 and the E-FEA exhibit remarkable similarity in the plastic zone, with a minor difference observed in the yield moment. Thus, it can be concluded that the claim made in [16] regarding the incompatibility between the experimental and E-FEA results in the plastic zone due to the use of elastically-perfect plastic steel plates in the E-FEA may not hold true. Therefore, it is imperative to identify and rectify the underlying source of this discrepancy.

3.4. Investigation of Discrepancies

3.4.1. Analysis of Yield Moment Deviation

The following observations were made:

(1) The yield stress of the steel plates reported in the experimental tests (Table 1) is higher than the yield stress used in the existing FE models (Table 2). However, Figure 5 shows that the E-FEA results display higher yield moments compared to the experimental results.
(2) The moment–rotation diagrams from FEA-2 (Figure 8), which employed the mechanical properties derived from the experimental tests, also indicate higher yield moments than the experimental results.
(3) A comparison between the specified minimum yield strength of Q345 steel plates (345 MPa) and the yield stress reported in the experimental tests (Table 1) shows that the reported yield stress is significantly higher than the specified minimum value. For example, for plate thicknesses up to 16 mm, the yield stress reported in the experimental tests is approximately 19% higher than the minimum yield strength. The reported average yield stress values for the steel plates in the experimental tests are obtained from tensile tests conducted on coupons. By contrast, the disparity between the specified minimum yield strength and the reported yield stress for bolts is smaller, as the latter values are derived directly from the bolt certificate of quality [15].
(4) Considering the high accuracy of linear analysis in advanced software such as ABAQUS, it is unlikely that the observed discrepancies in yield moments stem from software functionality. This is illustrated by the consistent agreement in the elastic zone slopes across all diagrams, including experimental tests, E-FEA, and FEA-2 results.

Based on the above observations, the discrepancies in yield moments can be attributed primarily to the reported yield strength values, which appear to be higher than their actual values. To investigate this, additional FE analyses were performed, confirming that the higher yield moments observed in the investigated connections (JD2, JD4, and JD6) are mainly due to the reported yield strength of the steel plates, while variations in bolt yield strength had no considerable effect.

It is important to note that the discrepancies in elastic behaviour—specifically in yield moments—are not the concern of this paper; instead, the main focus is on the plastic behaviour of the connections.

3.4.2. Analysis of Plastic Rotational Stiffness Deviation

This discrepancy can be attributed to the use of the elongation at rupture value as the strain corresponding to the ultimate stress in defining the plastic behaviour of steel plates and bolts, as discussed in Section 2.1. Although not explicitly stated in [16], the values in Table 2 clearly indicate that this approach was used for the bolts. Therefore, it is reasonable to assume that the same method was also applied to the steel plates. In FEA-1, which was conducted using mechanical properties equivalent to those in the E-FEA, the minimum elongation of 0.21 [25] was applied as the strain corresponding to the ultimate stress for

steel plates, while the elongation values for bolts were taken from Table 2. The results for FEA-1, shown in Figure 7, are in high agreement with the E-FEA results.

To further support the argument that the deviation in the E-FEA results, compared to experimental data, is primarily due to the utilisation of the elongation value as the strain corresponding to the ultimate stress, FEA-2 was conducted. The results for FEA-2, depicted in Figure 8, were obtained using mechanical properties equivalent to those reported in the experimental tests. However, similar to FEA-1, the minimum elongation was intentionally used as the strain corresponding to the ultimate stress for both steel plates and bolts (0.21 for steel plates [25], and 0.14 for bolts [28]). Despite the similarity in mechanical properties, the observed disparities between the experimental and FEA-2 results, along with the closer alignment of FEA-2 results with E-FEA results rather than the experimental results in the plastic zone, provide further evidence supporting the earlier claim.

For accurate analysis of the moment–rotation behaviour of connections, ABAQUS requires true stress–strain values. Therefore, either true stress–strain values must be directly available or engineering stress–strain values should be converted to true stress–strain values using mathematical relationships [34]. The use of engineering stress–strain data is identified as another contributing factor to the discrepancy between the experimental and E-FEA results in plastic rotational stiffness. In both FEA-1 and FEA-2, the mechanical properties were defined using engineering stress–strain values in ABAQUS. Based on the strong agreement between FEA-1 and the E-FEA results in the plastic zone, it can be inferred that engineering stress–strain values were adopted in the E-FEA.

As an illustrative example, to highlight the significant difference between the two data formats, the mechanical properties of steel plates with thicknesses less than 16 mm used in FEA-2 are considered. Their engineering ultimate stress and strain are 536.6 MPa and 0.21, respectively, whereas the corresponding true stress increases to 649.3 MPa and the true strain decreases to approximately 0.19.

Therefore, it can be concluded that the disparity in plastic rotational stiffness observed in the E-FEA and FEA-2 results is primarily due to the use of the minimum elongation or elongation at rupture reported in the experimental tests, combined with the use of engineering stress-strain values instead of true stress-strain values.

4. Results and Discussion

To enhance the accuracy of simulating the plastic behaviour of steel plates and bolts in order to minimize the discrepancies between FEA and experimental results, all connections were remodelled using the approximations described in Section 2.

4.1. Stress-Strain Approximation Methods and Effects

4.1.1. Multi-Linear Approximation

To address the underestimation of plastic rotational stiffness observed in the FEA results, new analyses were conducted under the same input conditions as FEA-2, with the following modifications applied individually:

- **FEA-3:** The plastic stress–strain behaviour of the steel plates and bolts was defined using the multi-linear approximation (Figure 2) and the linear approximation (a straight line connecting the yield and ultimate points), respectively.
- **FEA-4:** True stress–strain values were employed instead of engineering stress–strain values.
- **FEA-5:** A combination of FEA-3 and FEA-4, using true stress–strain values along with multi-linear and linear approximations for the plastic behaviour of the steel plates and bolts, respectively.

The comparison of results from FEA-2, FEA-3, FEA-4, and FEA-5 for the JD2 specimen is presented in Figure 9a–c.

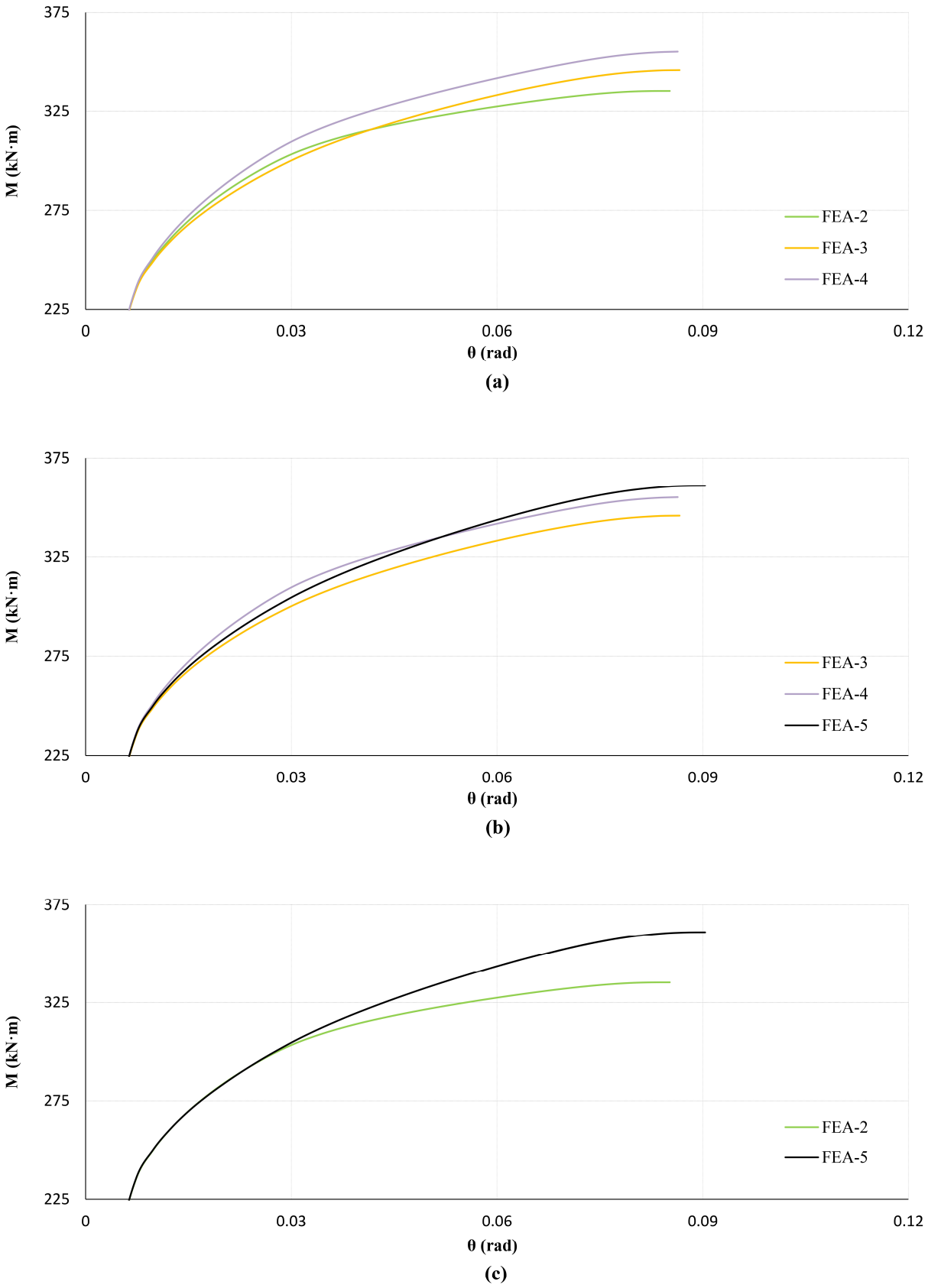


Figure 9. Comparison of different FEA results for the JD2 specimen.

Figure 9a shows that, at the onset of the plastic zone, moment values in FEA-3 are lower than those in FEA-2 (lower initial slope), whereas FEA-3 exhibits higher moment values at larger rotations (steeper slope). This behaviour is attributed to the use of multi-linear approximation, which accurately captures the initial region of plastic behaviour of the steel plates. This region, illustrated in Figure 2, spans from the yield strain up to a total strain of 0.02, where no stiffness is present. In contrast, FEA-4 results display a consistently higher slope throughout the plastic zone compared to FEA-2, reflecting the effect of employing true stress–strain values instead of engineering stress–strain values.

In Figure 9b, the moment values in FEA-5, which combines FEA-3 and FEA-4, are approximately the average of FEA-3 and FEA-4 at the onset of the plastic zone. At larger rotations, however, the FEA-5 curve exhibits noticeably higher moment values, indicating a significantly greater total plastic rotational stiffness compared to both FEA-3 and FEA-4.

Figure 9c compares the FEA-2 and FEA-5 curves, showing similar slopes at the onset of the plastic zone (up to 0.03 rad rotation), while FEA-5 exhibits a much steeper slope at larger rotations, indicating a significantly enhanced plastic rotational stiffness of the connection.

FEA-3, FEA-4, and FEA-5 were conducted for all specimens, with results shown in Figures 10–12 relative to FEA-2. The corresponding increase in plastic rotational stiffness (from 0.03 rad rotation onwards) is summarised in Table 3.

Table 3. Enhancement in plastic rotational stiffness of results in comparison to FEA-2.

FEA ID	Increase in Plastic Rotational Stiffness (%)						
	JD2	**JD3**	**JD4**	**JD6**	**JD7**	**JD8**	**Average**
FEA-3	39	27	17	35	50	30	33
FEA-4	39	19	31	30	45	35	33
FEA-5	61	36	43	52	76	53	53

Table 3 shows that defining the plastic behaviour of steel plates and bolts using multi-linear and linear approximations (FEA-3) has a similar effect on the results as replacing engineering stress–strain values with true stress–strain values (FEA-4), both showing a 33% increase in plastic rotational stiffness from 0.03 rad rotation onwards across all connections. The combination of these two measures (FEA-5) produces the highest effect, with an average increase of 53%. FEA-5 results are compared with experimental data in Figure 13, while the corresponding failure modes of all connections are shown in Figure 14.

Figure 13 shows strong agreement between FEA-5 results and experimental data for plastic rotational stiffness, with notable differences in the yield moments, particularly for the JD2, JD4, and JD6 specimens, which are attributed to the higher reported yield strength of the steel plates, as previously discussed.

An additional analysis, labelled "FEA-5-RYS" (Reduced Yield Strength), was performed for specimens with large discrepancies in yield moments. FEA-5-RYS uses the same input as FEA-5, with the only difference being that the mechanical properties of steel plates of all thicknesses were set equal to those of plates thicker than 16 mm, based on Table 1. While the ultimate strength of steel plates is nearly identical across thicknesses, their yield strengths differ; this adjustment reduces the yield strength of steel plates $\leq$ 16 mm by approximately 9%, from 409 MPa to 372.6 MPa. The results of FEA-5-RYS are presented in Figure 15 in comparison to experimental data.

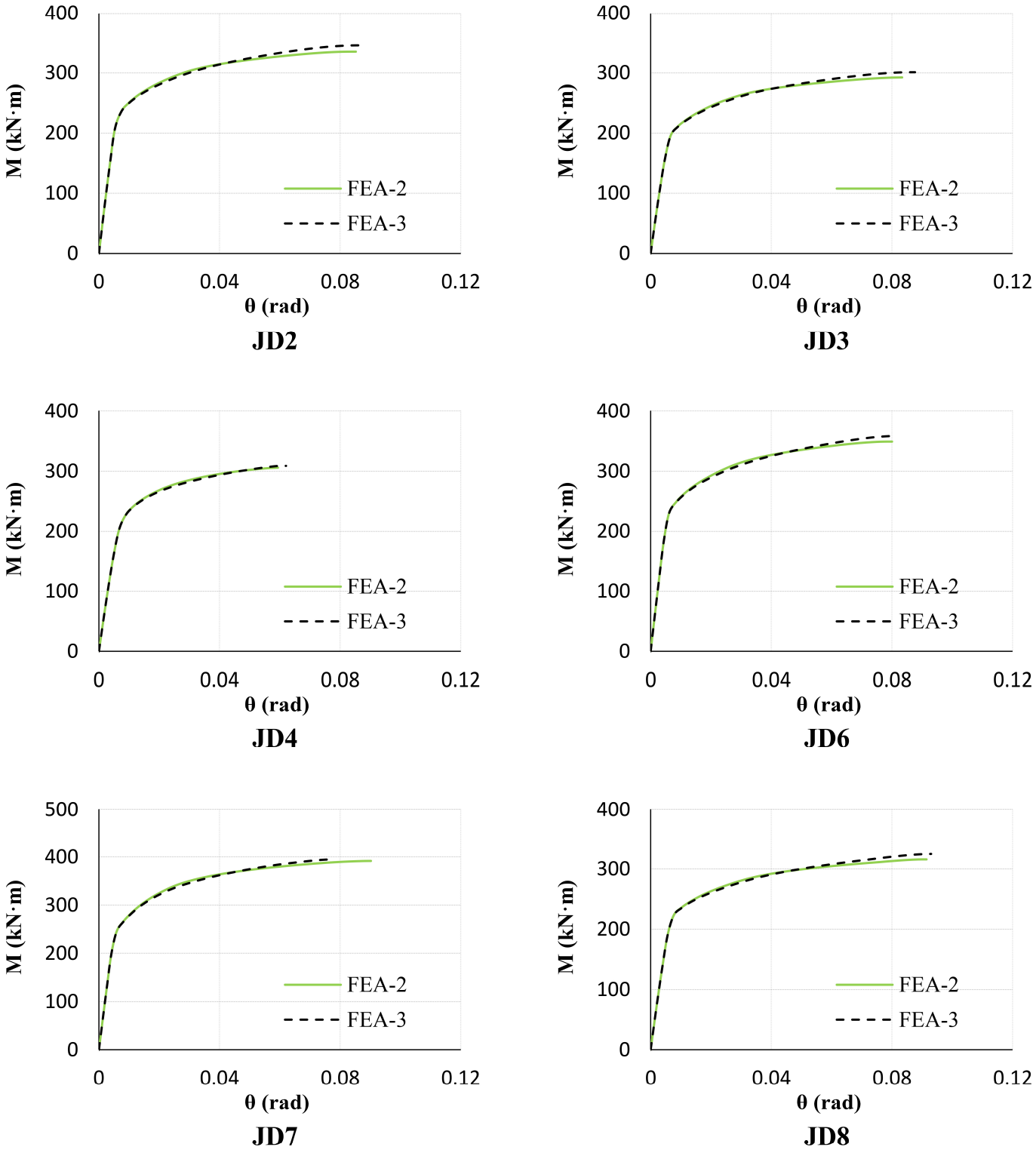


Figure 10. FEA results using minimum elongation as the strain corresponding to the ultimate stress (FEA-2), and FEA results using the multi-linear approximation (FEA-3).

Figure 15 shows very close agreement between FEA-5-RYS and experimental results in both the elastic and plastic zones, confirming that the remaining differences in FEA-5 results compared to experimental data (Figure 13) are solely due to the reported yield strength and not related to the FE simulations.

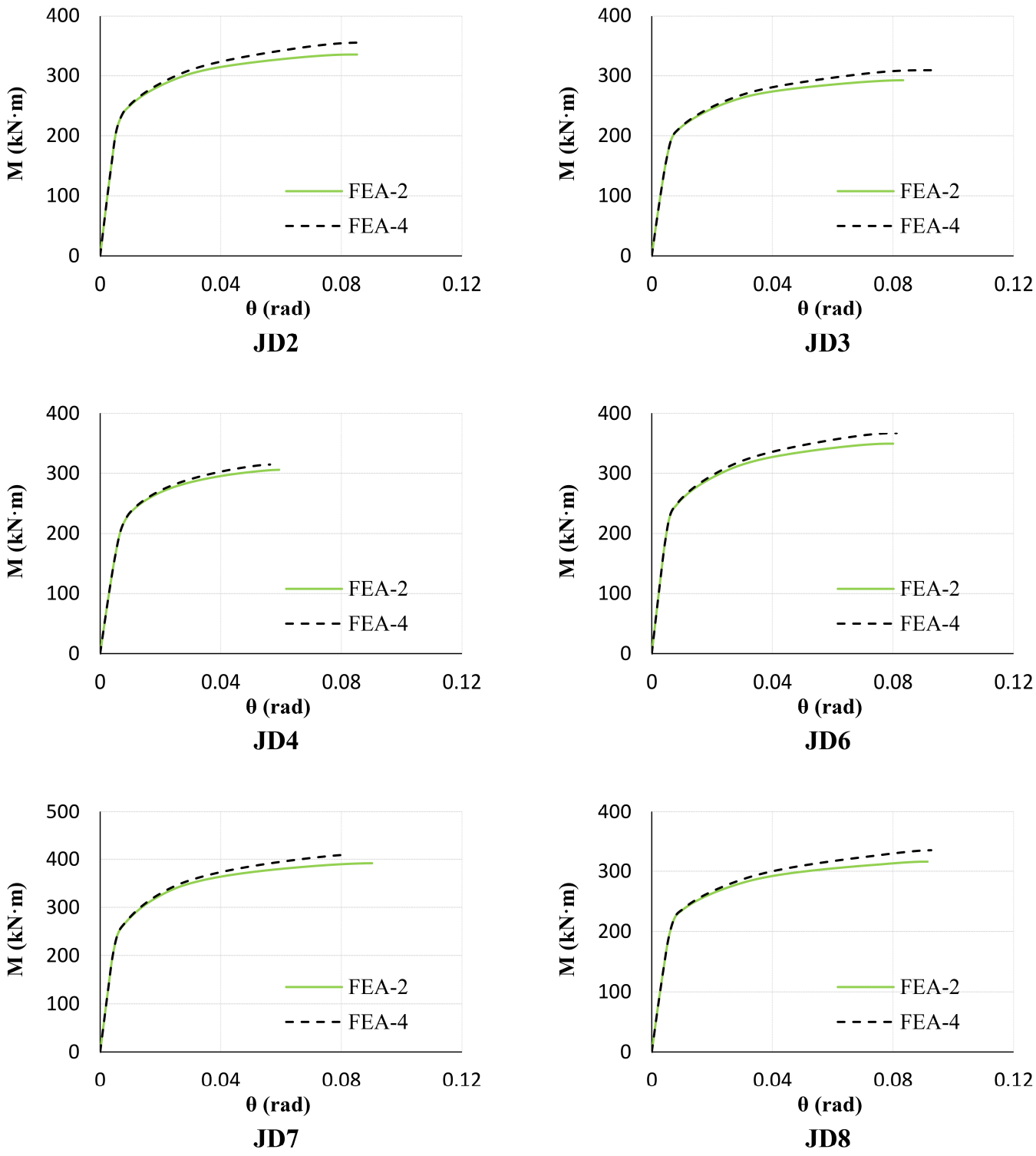


Figure 11. FEA results using engineering stress–strain values (FEA-2) and true stress–strain values (FEA-4).

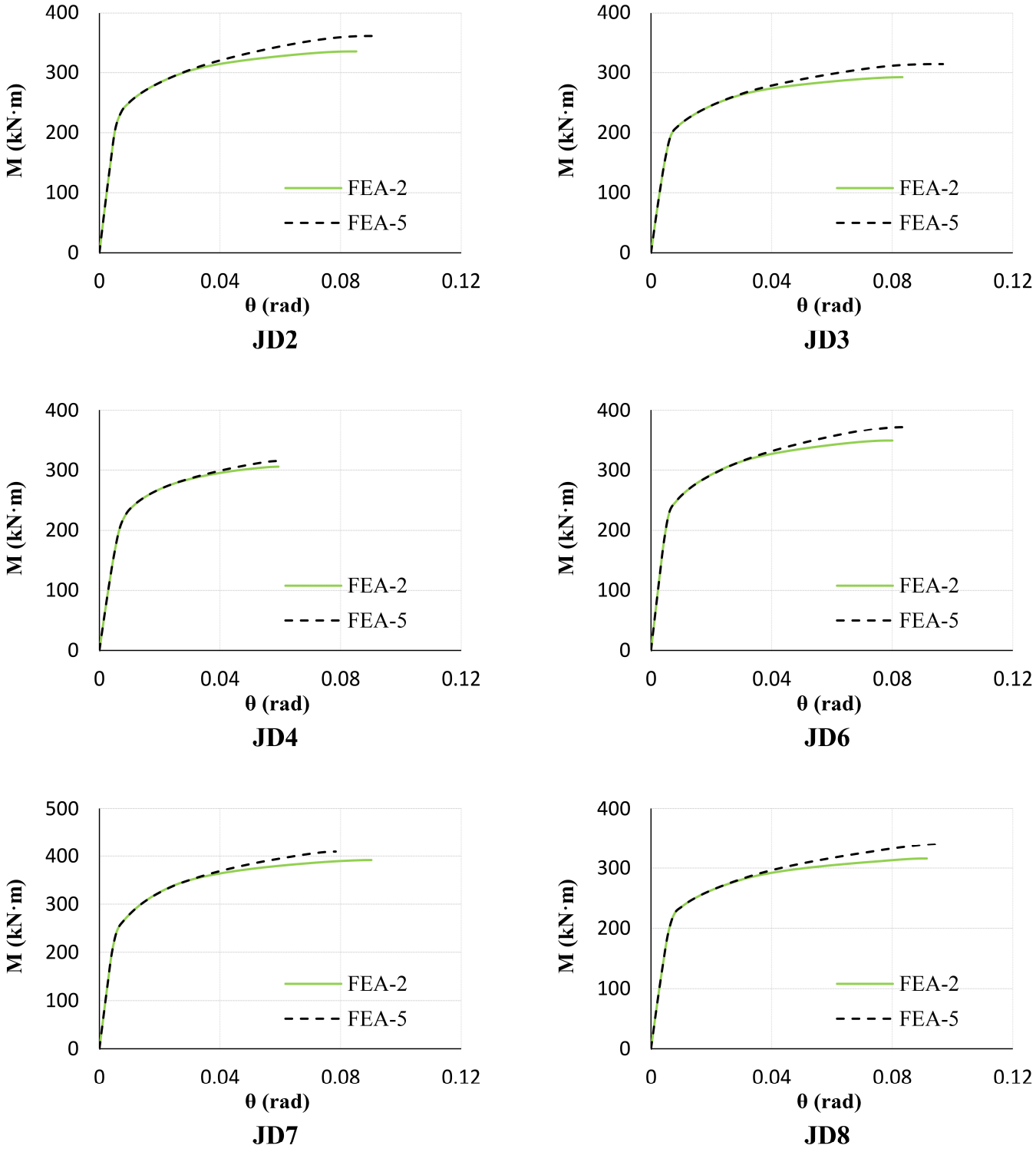


Figure 12. FEA results using minimum elongation as the strain corresponding to the ultimate stress along with engineering stress–strain values (FEA-2), and multi-linear approximation along with true stress–strain values (FEA-5).

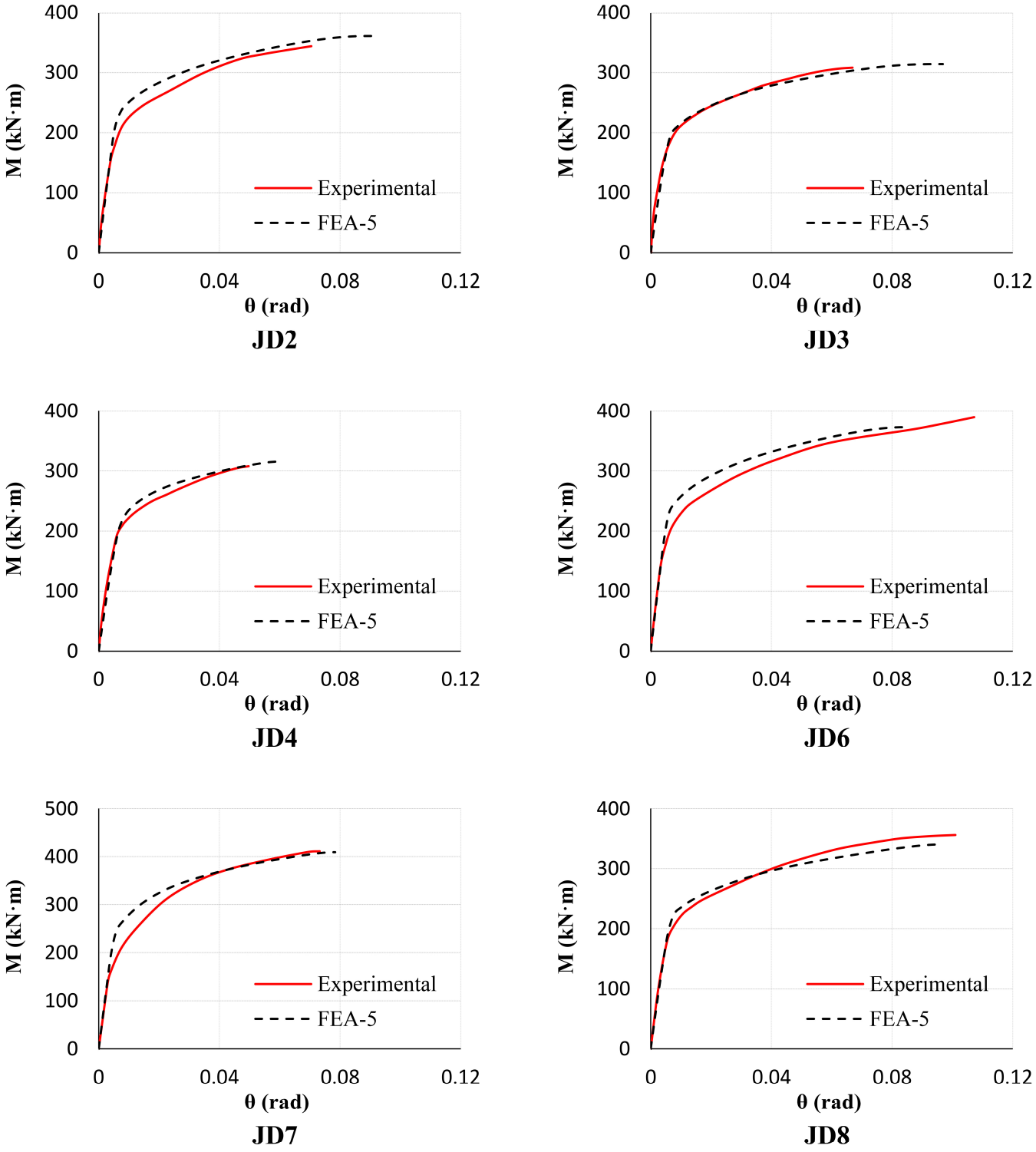


Figure 13. Experimental results [15] and FEA results using multi-linear approximation and true stress–strain values (FEA-5).

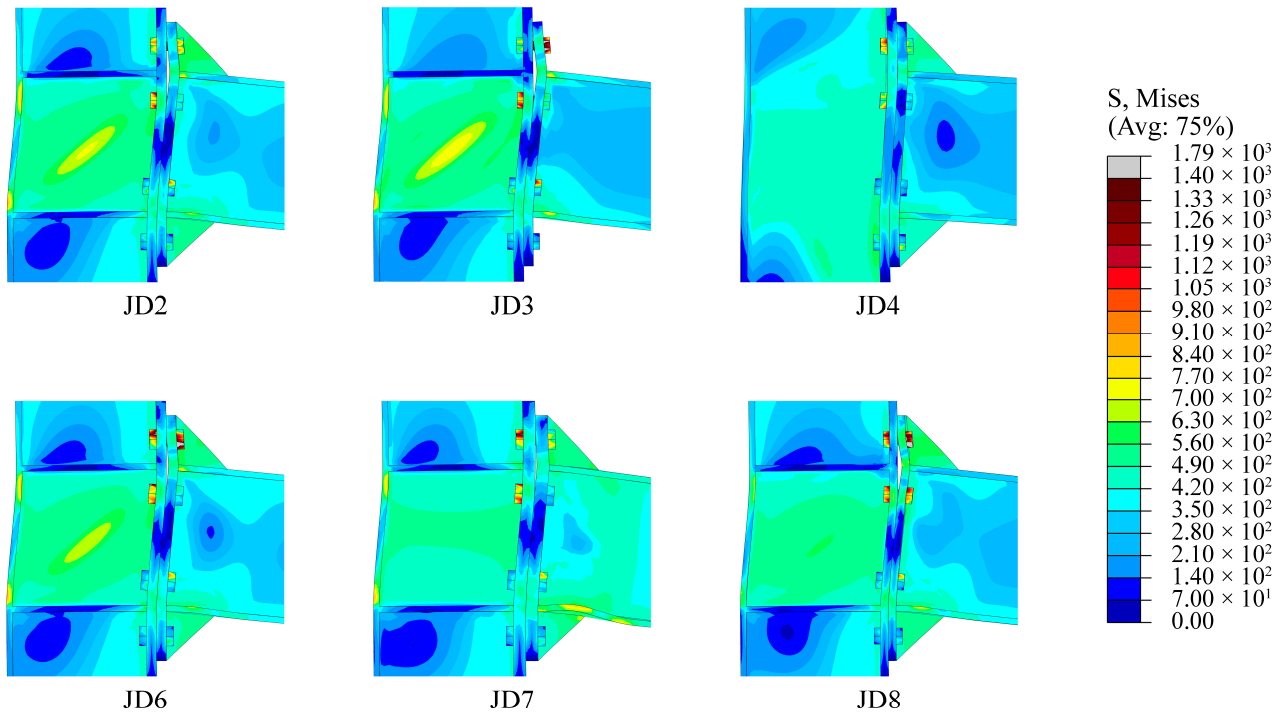


Figure 14. Comparison of connection failure modes in FEA-5.

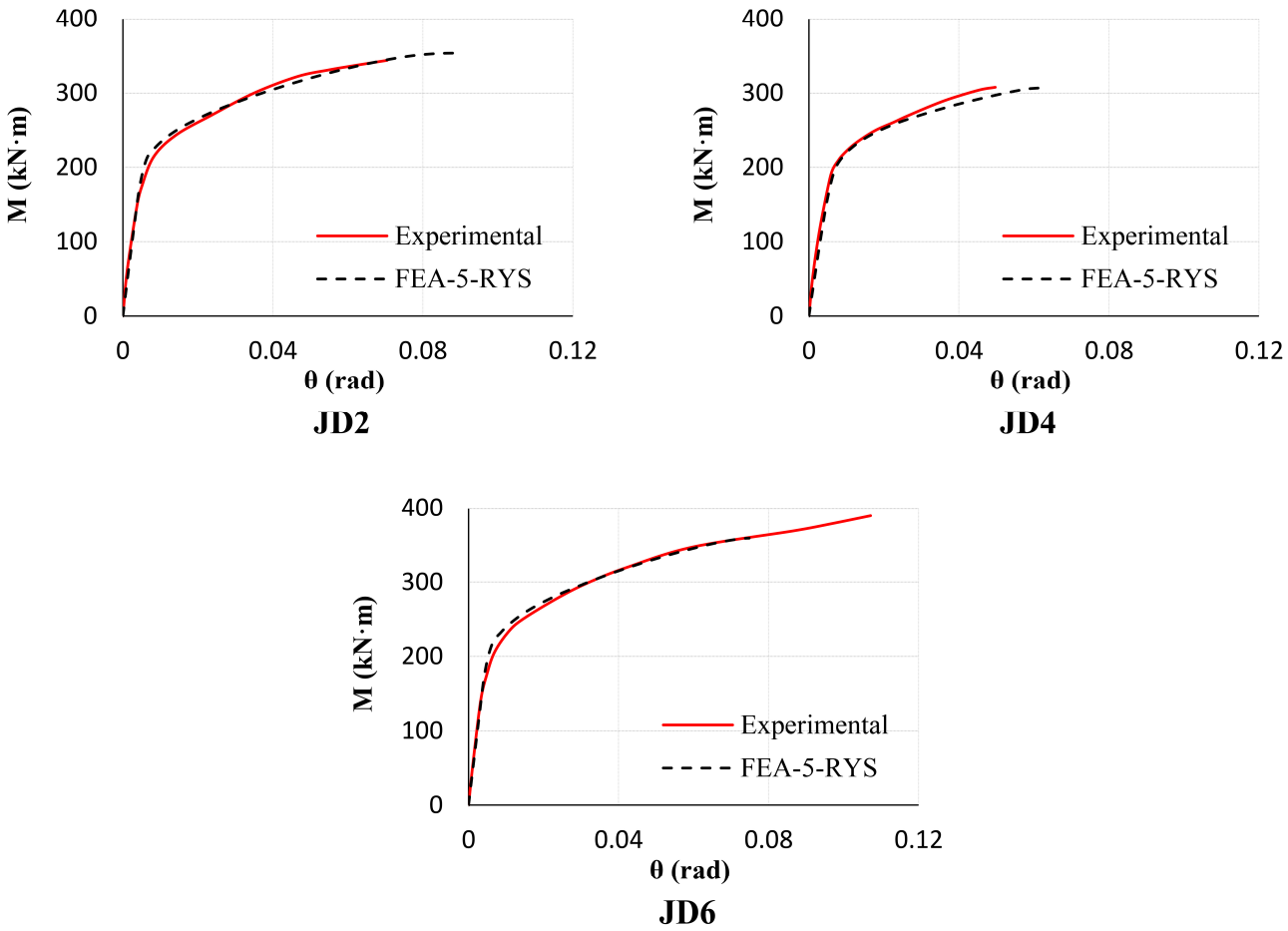


Figure 15. Experimental results [15] and FEA results with reduced yield strength of steel plates.

4.1.2. Bi-Linear Approximation

In situations where defining the plastic stress–strain behaviour of steel plates relies solely on the reported yield stress and ultimate stress values, a high level of agreement with experimental results can still be achieved. This can be accomplished by employing the bi-linear approximation method introduced in Section 2.1. The bi-linear approximation can be derived from either the actual stress–strain diagram or its multi-linear approximation.

In this paper, the proposed bi-linear approximation is constructed based on the multi-linear approximation shown in Figure 2. To develop this, the plastic region of the multi-linear diagram, specifically from the yield point to the ultimate point, is illustrated in Figure 16. The bi-linear approximation of the plastic stress–strain behaviour of steel plates, as depicted in Figure 16, is constructed in such a way that the areas under the multi-linear and bi-linear diagrams are equal.

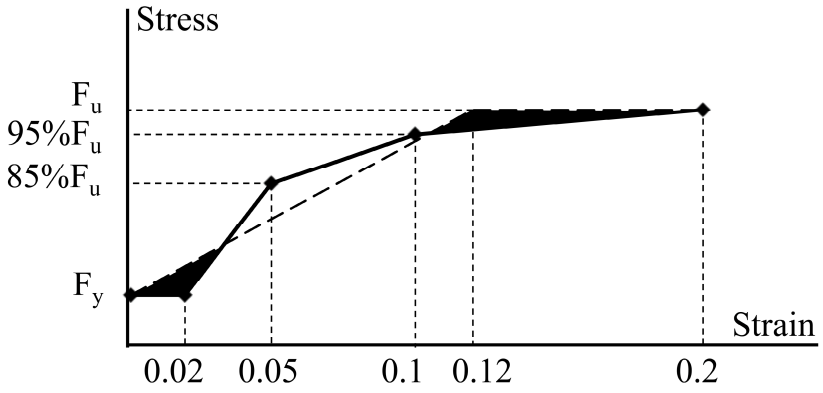


Figure 16. Bi-linear approximation for plastic stress–strain behaviour of mild steel.

As shown in Figure 16, the bi-linear approximation consists of three points: the yield point as the starting point (Point 1), the middle point (Point 2), and the ultimate point as the end point (Point 3). The start and end points of the bi-linear approximation are already known, as they coincide with the start and end points of the multi-linear approximation, respectively. The y-value of the middle point is also known and equals that of the end point. Thus, the only remaining unknown is the x-coordinate of the middle point (x_2).

In the following equations, (x_1, y_1), (x_2, y_2), and (x_3, y_3) correspond to the starting, middle, and end points of the bi-linear approximation, respectively.

To determine x_2, the area under the original diagram (A) is first calculated—either by integration or, in the case of a multi-linear curve, by simple mathematical expressions. The area under the bi-linear approximation is obtained from Equation (1), and equating it with the area under the original diagram allows x_2 to be determined using Equation (2).

$$A_{bi-linear} = \frac{1}{2}(x_2 - x_1)(y_2 + y_1) + (x_3 - x_2)y_3 \quad (1)$$

$$x_2 = \frac{(2A + x_1(y_3 + y_1) - 2x_3y_3)}{(y_1 - y_3)} \quad (2)$$

The strain value of 0.12 is determined as the strain corresponding to the ultimate stress. Beyond this point, up to a strain of 0.2, steel plates exhibit no further increase in strength.

In this step, all connections were reanalysed using true stress–strain values and the bi-linear approximation (Figure 16) and the linear approximation (a straight line connecting the yield and ultimate points) were employed to define the plastic stress–strain behaviour of steel plates and bolts, respectively. The results are presented in Figure 17 under the label "FEA-6".

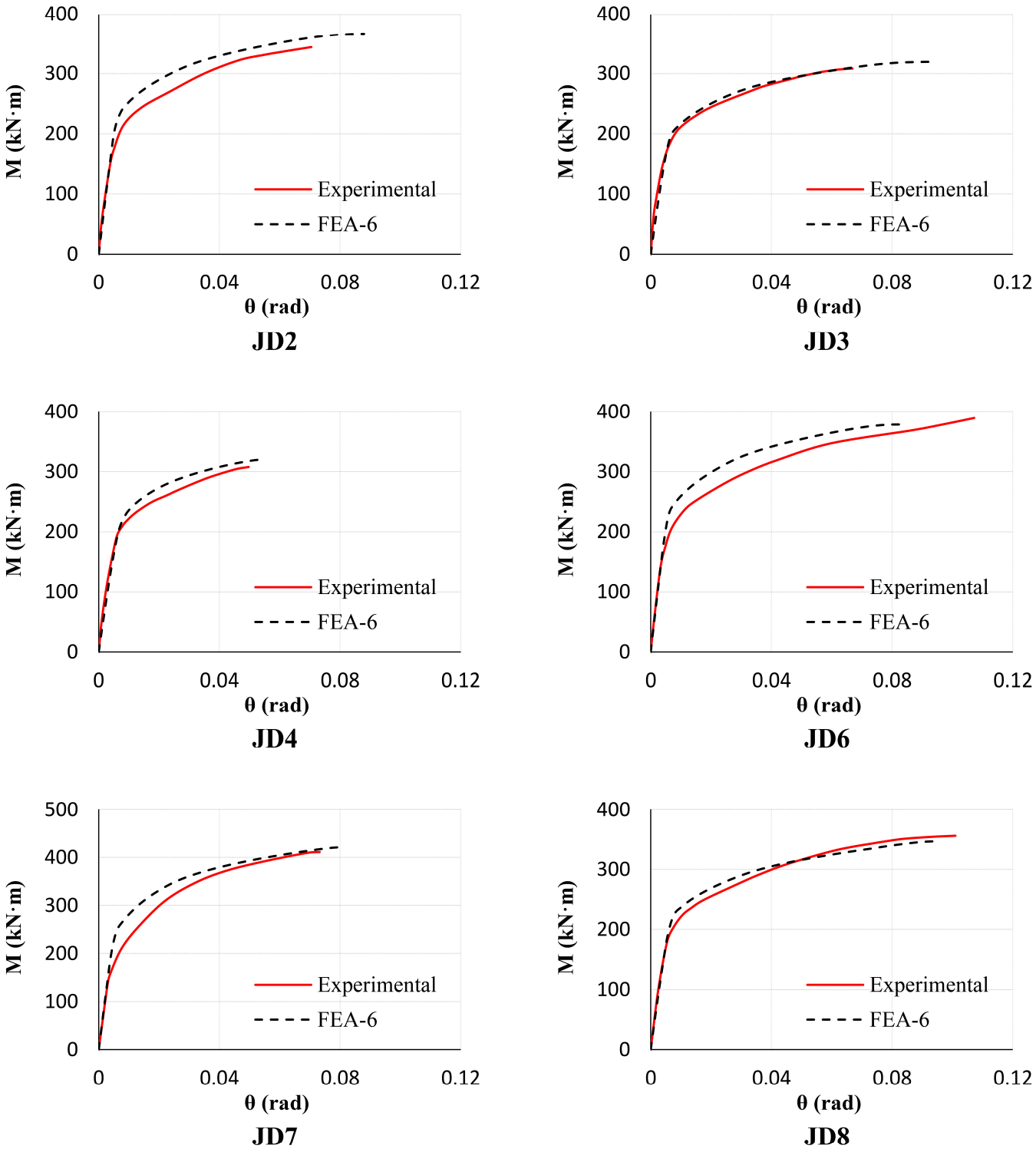


Figure 17. Experimental results [15] and FEA results using true stress–strain values and bi-linear approximation (FEA-6).

Figure 17 shows that FEA results using the bi-linear approximation for the plastic behaviour of steel plates are also in strong agreement with experimental data in terms of plastic rotational stiffness. In this approximation, the strain corresponding to the ultimate stress was determined as 0.12 (Figure 16), which is considerably lower than both the average ultimate strain (0.20 in Figure 2) and the minimum elongation (0.21) [25]. This explains why adopting either the average ultimate strain or the minimum elongation as the

strain corresponding to ultimate stress in a linear approximation (as in E-FEA and FEA-2) produces significant inaccuracies, particularly for mild steels.

4.2. Comparison of Plastic Rotational Stiffness

As previously mentioned, the primary difference between the experimental results and the existing FEA results for all connections lies in the slope of the moment–rotation diagram within the plastic zone, which reflects the plastic rotational stiffness of the connections. This stiffness was calculated for the experimental and FEA results based on their respective moment–rotation diagrams, starting from a rotation of 0.03 radians. The results are presented in Table 4.

Table 4. Plastic rotational stiffness of experimental and FEA results.

Analysis Type	Plastic Rotational Stiffness (kN·m/rad)					
	JD2	**JD3**	**JD4**	**JD6**	**JD7**	**JD8**
Experimental	1412	1177	1552	1231	1654	1097
E-FEA	671	693	888	542	873	545
FEA-2	718	678	856	697	853	573
FEA-5	1198	1051	1167	1057	1317	875
FEA-6	1142	1037	1210	1027	1300	884

The percent error of the plastic rotational stiffness for the FEA results, relative to the experimental results, was calculated for each connection. Additionally, the average percent error and the standard deviation of the percent errors were calculated for each type of FEA across all connections. The obtained values are presented in Table 5. To better illustrate these differences, Figure 18 presents a comparison of the plastic rotational stiffness deviations for each connection across different FEA results.

Table 5. Percent error of plastic rotational stiffness in FEA results with respect to experimental results.

FEA ID	Percent Error of Plastic Rotational Stiffness (%)							Standard Deviation (%)
	JD2	**JD3**	**JD4**	**JD6**	**JD7**	**JD8**	**Average**	
E-FEA	52	41	43	56	47	50	48	5.6
FEA-2	49	42	45	43	48	48	46	2.9
FEA-5	15	11	25	14	20	20	18	5.1
FEA-6	19	12	22	17	21	19	18	3.6

Table 5 shows that the average percent error for the existing FEA results, reported in [16], is 48%, and the percent error for the FEA-2 results—where engineering stress–strain values were used and no stress–strain approximations were applied—is 46%. In both cases, the deviation from the experimental results is significant.

The average percent errors for both FEA-5 and FEA-6 is 18%. In FEA-5, the plastic stress–strain behaviour of the steel plates was defined using the multi-linear approximation, whereas the bi-linear approximation was used in FEA-6. For both cases, the linear approximation was applied to define the plastic behaviour of the bolts and true stress–strain values were used instead of engineering values. The results indicate that using accurately implemented stress–strain approximations to define the plastic behaviour of the steel plates and bolts, together with the application of true stress–strain values, significantly enhances the accuracy of the FEA results.

The remaining 18% discrepancy in FEA-5 and FEA-6 results is attributed to material strain rehardening and the higher reported yield strength of the steel plates. Using a higher

yield stress with a fixed ultimate stress over the same strain span effectively reduces the simulated plastic stiffness. Table 5 shows that the smallest discrepancies occur for the JD3 specimen, where the difference in yield moments is marginal.

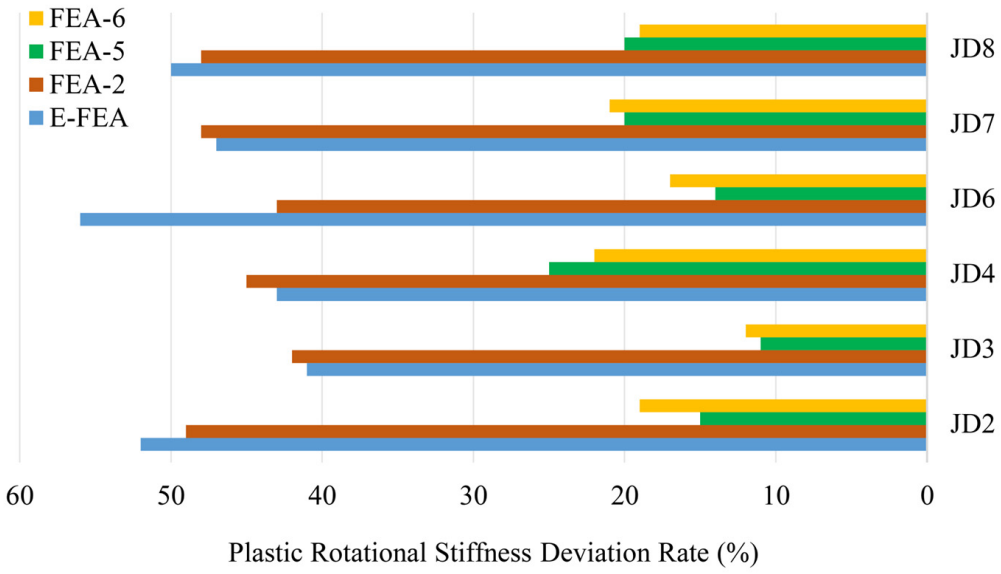


Figure 18. Comparison of plastic rotational stiffness deviations for each connection across different FEA results.

For E-FEA and FEA-2, although the standard deviations are relatively small (5.6% and 2.9%, respectively), the average percent errors are very large, indicating poor accuracy relative to the experimental results. This demonstrates that the errors are fairly consistent across all connections. For FEA-5 and FEA-6, the standard deviations (5.1% and 3.6%) are comparable to those of E-FEA and FEA-2, while their average percent errors are much lower. This indicates that these methods also maintain consistency across connections while achieving better agreement with experimental results. The standard deviation values therefore complement the average percent errors by providing insight into the stability of each FEA method across different connections.

4.3. Method Comparison and Applicability Analysis

If an accurate stress–strain diagram is available, the plastic behaviour can be defined directly using this diagram. However, experimental tests usually provide limited material data, primarily consisting of yield strength and ultimate strength values. Therefore, for a practical and reasonably accurate definition of mechanical properties, using a multi-linear approximation is an appropriate approach.

If a minimal-data approach is preferred, or if it is necessary to define the mechanical properties based solely on the yield and ultimate stress values, the plastic behaviour can be defined using the proposed bi-linear approximation.

It should be noted that the linear approximation of the plastic stress–strain behaviour (a straight line connecting the yield and ultimate points) is not suitable for mild steel, as it leads to significant discrepancies compared to the original stress–strain diagram due to the ductile nature of mild steel and the presence of large plastic strains near the ultimate stress. However, this linear approximation provides acceptable accuracy for defining the plastic behaviour of bolts, owing to their relatively brittle behaviour.

It is important to note that the appropriate data format for finite element modelling with any of these approaches—original diagram or any of the approximations—is the true stress–strain values.

Finally, the original stress–strain diagram offers the highest precision, whereas the linear approximation shows the lowest. Despite the general decrease in accuracy with fewer approximation points, the bi-linear approximation yields comparable results to the multi-linear approximation regarding plastic rotational stiffness.

A summary of these considerations is presented in Table 6.

Table 6. Recommended modelling strategy for different levels of material data availability.

Material Data Availability	Recommended Modelling Strategy	Data Format for FEA
Complete stress–strain diagram	Complete stress–strain diagram	True stress–strain
Yield and ultimate stress (mild steel)	Multi-linear approximation	True stress–strain
Yield and ultimate stress (minimal-data approach, mild steel)	Bi-linear approximation	True stress–strain
Yield and ultimate stress (ASTM A490M/Grade 10.9 bolts)	Linear approximation	True stress–strain

5. Conclusions

This study re-examined the finite element analysis (FEA) of bolted extended end-plate beam-to-column moment connections with the specific aim of understanding and improving the prediction of plastic rotational stiffness through more rigorous material modelling. Six experimentally tested connections (JD2, JD3, JD4, JD6, JD7, JD8) were re-modelled in ABAQUS, the existing numerical model from the literature was independently reproduced, and a series of refined stress–strain approximations—multi-linear and bi-linear—were developed and implemented using true stress–strain input. On this basis, the following conclusions, limitations and future research directions are drawn.

6. Key Findings and Outcomes

1. Stress–strain definition and data format are the dominant drivers of error.

Comparison of the experimental curves with the existing FEA (E-FEA) and with the reproduced model using experimental mechanical properties (FEA-2) showed that the average error in plastic rotational stiffness was of the order of 46–48%. This is because the models included only the measured yield and ultimate strengths, without specifying the stress–strain curve shape and format. The principal causes of the discrepancy were identified as:

- The use of engineering stress–strain data instead of true stress–strain values in the FE material definitions;
- The use of a single linear plastic branch extending to the minimum elongation or an average ultimate strain, which produces an unrealistically long and shallow plastic range for mild structural steel.

2. Multi-linear approximations significantly improve plastic stiffness predictions.

Employing a multi-linear approximation for the plastic behaviour of mild steel plates [26] and a linear plastic branch for grade 10.9 bolts, while still using engineering stress–strain values (FEA-3), increased the average plastic rotational stiffness by approximately 33% relative to FEA-2. This demonstrates that the shape of the stress–strain curve in the plastic range has a substantial influence on the predicted moment–rotation response.

3. Using true instead of engineering stress–strain values has a comparable quantitative effect.

Reformulating the material input so that the same curve shapes were supplied to ABAQUS in terms of true stress and logarithmic plastic strain (FEA-4), without utilising

stress–strain approximations, produced a similar 33% average increase in plastic rotational stiffness compared with FEA-2. Thus, the data format (engineering vs. true) is as important as the curve shape when modelling large plastic deformations in extended end-plate moment connections.

4. The combined multi-linear + true stress–strain strategy provides robust agreement with experiments.

When multi-linear approximations for steel plates and linear approximations for bolts were combined with true stress–strain input (FEA-5), the average plastic rotational stiffness increased by about 53% relative to FEA-2. The resulting moment–rotation curves matched the experimental behaviour well in the plastic range for all six connections. This combined approach reduces the average stiffness error from about 46–48% (E-FEA, FEA-2) to approximately 18%, representing a substantial improvement in modelling accuracy.

5. Bi-linear approximations offer a practical and accurate alternative when data are limited.

For situations in which only yield strength, ultimate strength, and a global elongation measure are available, a bi-linear approximation was formulated by enforcing equality of the area under the bi-linear and reference stress–strain curves between yield and ultimate strain. Implemented with true stress–strain values (FEA-6), this bi-linear strategy yielded plastic rotational stiffness predictions that were essentially comparable to those of FEA-5, with an average error of about 18% relative to experiments. The bi-linear model therefore provides a practical, data-efficient approach for design-oriented FEA when full stress–strain curves are not reported.

6. Different treatment is required for mild steels and high-strength bolts.

The study confirms that a single linear plastic branch is inadequate for representing the plastic behaviour of mild structural steels (e.g., Q345/ASTM A572 Gr50) used in plates, as it significantly distorts both plastic stiffness and energy absorption. In contrast, for grade 10.9 high-strength bolts (ASTM A490M) with a short and steep plastic range and limited ductility, a single linear approximation between yield and ultimate stresses was found to be sufficient for monotonic loading, as the differences in area and stiffness relative to a more detailed curve are small.

7. Residual discrepancies are primarily linked to yield strength uncertainty and strain hardening.

Even with refined multi-linear and bi-linear approximations and true stress–strain input (FEA-5 and FEA-6), an average residual error of about 18% remained. A sensitivity analysis in which the yield strength of thin plates was slightly reduced (FEA-5-RYS) produced very close agreement with the experimental curves, indicating that the remaining discrepancies are largely attributable to:

- Uncertainty and variability in the actual yield strength of the steel plates;
- Simplified representation of strain hardening and re-hardening in the adopted approximations.

Thus, once the stress–strain curve shape and data format are defined correctly, yield strength variability becomes the dominant source of modelling error.

7. Practical Implications and Modelling Recommendations

The findings of this study lead to several practical recommendations for researchers and practitioners performing FEA of extended end-plate and similar steel connections:

- Always use true stress–strain input for plasticity in ABAQUS (and similar FE codes) and avoid using engineering stress–strain curves directly in the material definition for large-deformation analyses.
- Do not take minimum elongation or average ultimate strain as the strain at ultimate stress in a single linear plastic branch for mild steels; this practice leads to excessive plastic strain range and systematically underestimates plastic rotational stiffness.
- When detailed stress–strain data or reliable reference diagrams are not available, adopt a multi-linear approximation for mild steel plates and a linear approximation for high-strength bolts.
- When only yield and ultimate strengths are known, construct a bi-linear approximation whose plastic energy is matched to an appropriate reference curve or to test data; use this bi-linear law with true stress–strain input.
- Treat bolts and plates differently in material modelling: multi-/bi-linear laws for plates and a simple linear plastic law for high-strength bolts are appropriate for monotonic analyses.

These recommendations provide a transferable modelling framework that can be adopted in future parametric studies and in design-oriented finite element simulations of steel connections.

8. Limitations

The scope and assumptions of the present work impose several limitations that should be acknowledged:

1. Restricted connection typology and test database.

The calibration and validation are based on a single experimental programme of eight extended end-plate connections, of which six were considered in the detailed numerical study. All specimens share a similar overall configuration (beam-to-column, extended end-plate, grade 10.9 bolts) and material grade. The conclusions are therefore most directly applicable to similar joint types and may require further verification for markedly different geometries or detailing (e.g., flush end-plates, partial-strength joints, composite slab effects).

2. Monotonic loading only.

All tests and simulations were carried out under monotonic loading. Cyclic degradation, pinching, low-cycle fatigue, and cumulative damage under seismic-type loading were not modelled. The suitability of the multi-linear and the proposed bi-linear laws for cyclic or seismic analyses remains to be investigated.

3. Material models focused on monotonic plasticity.

The adopted material laws consider isotropic hardening in monotonic loading and do not explicitly treat phenomena such as Bauschinger effect, kinematic hardening, or ratcheting. These effects may become important in cyclic loading or in cases with significant load reversals.

4. Generalisability to other steels and connection details.

The study focused on mild structural steel (similar to Q345/ASTM A572 Gr50) and grade 10.9 bolts. The same approximations may not be directly applicable to high-strength steels, stainless steels, or steels with markedly different strain-hardening characteristics without recalibration.

5. Modelling assumptions beyond material behaviour.

Although the finite element model was carefully constructed and validated against published results, some modelling choices—such as mesh density, contact modelling,

friction coefficients, residual stress representation, and boundary conditions—were not exhaustively varied in a systematic sensitivity study. These aspects may also influence the predicted rotational stiffness and should be considered when transferring the modelling procedure to other problems.

9. Future Research Directions

Building on the present findings, several avenues for further investigation are apparent:

1. Extension to other connection types and composite systems.

Future work should apply and validate the proposed material modelling strategy for a broader range of joint configurations, including flush end-plate connections, double-angle and T-stub connections, minor-axis joints, and composite beam–column assemblies with concrete slabs and decking. This would help to establish the generality of the approach and its integration into component-based design methods.

2. Cyclic and seismic loading, low-cycle fatigue and fracture.

The refined multi-/bi-linear models should be extended to account for cyclic behaviour, including kinematic hardening, stiffness and strength degradation, and low-cycle fatigue. Experimental data from cyclic tests could be used to calibrate and validate cyclic material models and to study fracture initiation and propagation in end-plates and bolts under seismic loading.

3. Parametric studies and simplified design models.

With the improved material modelling framework, extensive parametric studies can be conducted to quantify the influence of parameters such as plate thickness, bolt diameter and grade, end-plate extension, bolt pre-tension, and axial force level on connection stiffness, strength, and ductility. The results can then be synthesised into simplified rotational spring models, component-based formulations, or design charts for routine structural analysis and code calibration.

4. Calibration for other steel grades and technologies.

The multi-linear and bi-linear strategies can be adapted and re-calibrated for high-strength steels, stainless steels and advanced materials used in modern steel construction. This may include characterisation of strain hardening, local necking behaviour, and temperature effects, with a view to extending the approach to fire and robustness assessments.

5. Uncertainty quantification and reliability-based design.

Given the demonstrated sensitivity to yield strength variability, future work could integrate the proposed modelling framework with probabilistic methods, such as Monte Carlo simulation or reliability analysis, to quantify the impact of material and geometric variability on connection performance and to inform reliability-based design and partial factor calibration.

6. Automated identification of optimal approximations from test data.

Finally, optimisation techniques and machine learning tools could be employed to automatically derive multi-linear or bi-linear stress–strain curves from experimental data that best reproduce key connection response metrics (e.g., initial stiffness, plastic stiffness, rotation capacity). Such procedures could further standardise and streamline the calibration of material models for connection FEA.

7. Extension to nonlinear dynamic and fire analysis.

Future research should extend the proposed method to nonlinear dynamic analysis and fire conditions, enabling a more comprehensive assessment of structural performance

under complex loading and environmental scenarios. Such studies would further clarify the applicability of the method beyond monotonic and cyclic loading regimes.

In summary, the study demonstrates that carefully constructed multi-linear and bi-linear stress–strain approximations, implemented with true stress–strain input, provide a robust and practical basis for accurately predicting the plastic rotational stiffness of bolted extended end-plate moment connections. The work offers both specific quantitative improvements for the tested joints and a general modelling framework that can support more reliable and efficient numerical investigation of steel connection behaviour in future research and design practice.

Author Contributions: Conceptualization, I.R. and M.R.T.; Methodology, I.R.; Software, I.R.; Validation, I.R.; Formal analysis, I.R.; Investigation, I.R.; Resources, I.R. and R.E.; Data curation, I.R.; Writing—original draft, I.R. and R.E.; Writing—review and editing, I.R. and S.B.; Visualization, I.R.; Supervision, M.R.T.; Project administration, M.R.T. All authors have read and agreed to the published version of the manuscript.

Funding: This research received no external funding.

Data Availability Statement: The original data presented in the study are openly available in Mendeley Data at [33].

Acknowledgments: We sincerely thank Ehsan Rahchamandi for his support and valuable assistance.

Conflicts of Interest: The authors declare no conflicts of interest.

References

1. Eatherton, M.R.; Murray, T.M. *Design Guide 39: End-Plate Moment Connections*; American Institute of Steel Construction: Chicago, IL, USA, 2023. Available online: https://aisc.org/products/publication/design-guides/design-guide-39-end-plate-moment-connections (accessed on 28 November 2025).
2. *AISC 341-22*; Seismic Provisions for Structural Steel Buildings. AISC: Chicago, IL, USA, 2022. Available online: https://aisc.org/Seismic-Provisions-for-Structural-Steel-Buildings-ANSIAISC-341-22-Download (accessed on 28 November 2025).
3. *AISC 358-22*; Prequalified Connections for Special and Intermediate Steel Moment Frames for Seismic Applications. AISC: Chicago, IL, USA, 2022. Available online: https://aisc.org/products/publication/standards/aisc-358/prequalified-connections-for-special-and-intermediate-steel-moment-frames-for-seismic-applications (accessed on 28 November 2025).
4. Abidelah, A.; Bouchaïr, A.; Kerdal, D.E. Experimental and analytical behavior of bolted end-plate connections with or without stiffeners. *J. Constr. Steel Res.* **2012**, *76*, 13–27. [CrossRef]
5. Díaz, C.; Victoria, M.; Martí, P.; Querin, O.M. FE model of beam-to-column extended end-plate joints. *J. Constr. Steel Res.* **2011**, *67*, 1578–1590. [CrossRef]
6. ElSabbagh, A.; Sharaf, T.; Nagy, S.; ElGhandour, M. Behavior of extended end-plate bolted connections subjected to monotonic and cyclic loads. *Eng. Struct.* **2019**, *190*, 142–159. [CrossRef]
7. Mashaly, E.; El-Heweity, M.; Abou-Elfath, H.; Osman, M. Finite element analysis of beam-to-column joints in steel frames under cyclic loading. *Alex. Eng. J.* **2011**, *50*, 91–104. [CrossRef]
8. Krishnamurthy, N.; Graddy, D.E. Correlation between 2- and 3-dimensional finite element analysis of steel bolted end-plate connections. *Comput. Struct.* **1976**, *6*, 381–389. [CrossRef]
9. Bahaari, M.R.; Sherbourne, A.N. Computer modelling of an extended end-plate bolted connection. *Comput. Struct.* **1994**, *52*, 879–893. [CrossRef]
10. Sherbourne, A.N.; Bahaari, M.R. 3D simulation of end-plate bolted connections. *J. Struct. Eng.* **1994**, *120*, 3122–3136. [CrossRef]
11. Bahaari, M.R.; Sherbourne, A.N. Structural behavior of end-plate bolted connections to stiffened columns. *J. Struct. Eng.* **1996**, *122*, 926–935. [CrossRef]
12. Bahaari, M.R.; Sherbourne, A.N. 3D simulation of bolted connections to unstiffened columns—II. Extended endplate connections. *J. Constr. Steel Res.* **1996**, *40*, 189–223. [CrossRef]
13. Bursi, O.S.; Jaspart, J.P. Calibration of a finite element model for isolated bolted end-plate steel connections. *J. Constr. Steel Res.* **1997**, *44*, 225–262. [CrossRef]
14. Maggi, Y.I.; Gonçalves, R.M.; Leon, R.T.; Ribeiro, L.F.L. Parametric analysis of steel bolted end plate connections using finite element modeling. *J. Constr. Steel Res.* **2005**, *61*, 689–708. [CrossRef]

15. Shi, G.; Shi, Y.; Wang, Y. Behaviour of end-plate moment connections under earthquake loading. *Eng. Struct.* **2007**, *29*, 703–716. [CrossRef]
16. Shi, G.; Shi, Y.; Wang, Y.; Bradford, M.A. Numerical simulation of steel pretensioned bolted end-plate connections of different types and details. *Eng. Struct.* **2008**, *30*, 2677–2686. [CrossRef]
17. Bai, R.; Chan, S.-L.; Hao, J.-P. Improved design of extended end-plate connection allowing for prying effects. *J. Constr. Steel Res.* **2015**, *113*, 13–27. [CrossRef]
18. Augusto, H.; Simões da Silva, L.; Rebelo, C.; Castro, J.M. Cyclic behaviour characterization of web panel components in bolted end-plate steel joints. *J. Constr. Steel Res.* **2017**, *133*, 310–333. [CrossRef]
19. Dinu, F.; Marginean, I.; Dubina, D. Experimental testing and numerical modelling of steel moment-frame connections under column loss. *Eng. Struct.* **2017**, *151*, 861–878. [CrossRef]
20. Tartaglia, R.; D'Aniello, M.; Rassati, G.A.; Swanson, J.A.; Landolfo, R. Full strength extended stiffened end-plate joints: AISC vs recent European design criteria. *Eng. Struct.* **2018**, *159*, 155–171. [CrossRef]
21. Tartaglia, R.; D'Aniello, M.; Landolfo, R. The influence of rib stiffeners on the response of extended end-plate joints. *J. Constr. Steel Res.* **2018**, *148*, 669–690. [CrossRef]
22. Eladly, M.M.; Schafer, B.W. Numerical and analytical study of stainless steel beam-to-column extended end-plate connections. *Eng. Struct.* **2021**, *240*, 112392. [CrossRef]
23. Krolo, P.; Grandić, D. Hysteresis envelope model of double extended end-plate bolted beam-to-column joint. *Buildings* **2021**, *11*, 517. [CrossRef]
24. Nie, S.; Chen, S.; Wu, W.; Jiang, X.; Wang, S.; Lin, Y.; Liu, M. An investigation on the seismic behavior of the end-plate connection between a steel beam and the weak-axis of an H-shaped column using a U-shaped connector. *Buildings* **2024**, *14*, 1087. [CrossRef]
25. *ASTM A572/A572M-21e1*; Standard Specification for High-Strength Low-Alloy Columbium-Vanadium Structural Steel. ASTM International: West Conshohocken, PA, USA, 2021. [CrossRef]
26. Rex, C.O.; Easterling, W.S. *Behavior and Modeling of Mild and Reinforcing Steel*; Report No. CE/VPI-ST 96/12; Virginia Polytechnic Institute and State University: Blacksburg, VA, USA, 1996. Available online: https://www.aisc.org/globalassets/aisc/research-library/behavior-and-modeling-of-mild-and-reinforcing-steel.pdf (accessed on 28 November 2025).
27. *ASTM A490M-12*; Standard Specification for High-Strength Steel Bolts, Classes 10.9 and 10.9.3, for Structural Steel Joints (Metric). ASTM International: West Conshohocken, PA, USA, 2012. [CrossRef]
28. *ASTM F3125/F3125M-23*; Standard Specification for High Strength Structural Bolts and Assemblies, Steel and Alloy Steel, Heat Treated, Inch Dimensions 120 ksi and 150 ksi Minimum Tensile Strength, and Metric Dimensions 830 MPa and 1040 MPa Minimum Tensile Strength. ASTM International: West Conshohocken, PA, USA, 2023. [CrossRef]
29. Kulak, G. *Design Guide 17: High Strength Bolts: A Primer for Structural Engineers*; American Institute of Steel Construction: Chicago, IL, USA, 2002. Available online: https://aisc.org/Design-Guide-17-High-Strength-Bolts-A-Primer-for-Structural-Engineers (accessed on 28 November 2025).
30. Hashemi Rezvani, F.; Ronagh, H. Span length effect on alternate load path capacity of welded unreinforced flange-bolted web connections. *J. Constr. Steel Res.* **2017**, *138*, 714–728. [CrossRef]
31. RCSC. *Specification for Structural Joints Using High-Strength Bolts*; RCSC: Chicago, IL, USA, 2020. Available online: https://boltcouncil.org/documents.html (accessed on 28 November 2025).
32. *ASME B18.2.6M-12*; Metric Fasteners for Use in Structural Applications. American Society of Mechanical Engineers: New York, NY, USA, 2012. Available online: https://asme.org/codes-standards/find-codes-standards/b18-2-6m-metric-fasteners-use-structural-applications/2012/pdf (accessed on 28 November 2025).
33. Rahchamandi, I.; Tavassoli, M.R.; Esmaeilabadi, R.; Banihashemi, S. *Dataset for ABAQUS Modelling of Beam-to-Column Bolted Extended End-Plate Moment Connections Using Stress–Strain Approximations*; V1; Mendeley Data; 2026. [CrossRef]
34. Dassault Systèmes Simulia Corp. *ABAQUS 6.14 Analysis User's Guide*; Volume 3: Materials; Dassault Systèmes Simulia Corp.: Providence, RI, USA, 2014; p. 23.1.1-6.

Disclaimer/Publisher's Note: The statements, opinions and data contained in all publications are solely those of the individual author(s) and contributor(s) and not of MDPI and/or the editor(s). MDPI and/or the editor(s) disclaim responsibility for any injury to people or property resulting from any ideas, methods, instructions or products referred to in the content.